

OMEGACAM

User Manual

OmegaCAM Instrument Consortium

Document Number:

VST-MAN-OCM-23100-3110

Issue Number:

2.7.1

Issue Date:

14.09.2011

Author:

K. Kuijken

| Distribution List | | |
|--------------------------|---------------------|---------------|
| Recipient | Institute / Company | No. of Copies |
| D. Baade | ESO | 1 |

| Document Change Record | | | |
|-------------------------------|------------|----------------------------|---|
| Issue | Date | Sect. / Paragr. affected | Reasons / Remarks |
| 1.0 | 31.03.2004 | all | first issue (PAE) |
| 1.1 | 13.05.2004 | most | changes in response to first RIXes (DBA, RHA) |
| 2.0 draft | 20.12.2006 | Appendix | small textual changes Laboratory measurements of filter throughput |
| 2.5 | 26.06.2011 | | update based on commissioning |
| 2.6 | 11.08.2011 | 2.3 | updates on filter naming and characteristics |
| 2.7 | 05.09.2011 | many, note 3.2.2 and 3.4.4 | Update by ESO-PSO after science verification |
| 2.7.1. | 14.09.2011 | | Minor language updates by ESO-USD |

Contents

| | | |
|----------|---|-----------|
| 1 | Introduction | 1 |
| 1.1 | Scope | 1 |
| 1.2 | More Info | 1 |
| 1.3 | References | 1 |
| 1.4 | Acronyms | 1 |
| 2 | Instrument characteristics | 3 |
| 2.1 | Overview | 3 |
| 2.2 | Detector Mosaic | 6 |
| 2.2.1 | The 268-Million Pixel Science Array | 6 |
| 2.2.2 | Auxiliary CCDs | 12 |
| 2.3 | Filters | 14 |
| 2.3.1 | Note on filter magazines | 15 |
| 2.3.2 | Providing Private Filters | 17 |
| 2.4 | Shutter | 17 |
| 2.5 | Auto-Guiding and Focussing | 18 |
| 2.5.1 | VST Guide Probe | 18 |
| 2.5.2 | Auto-guiding with OmegaCAM | 19 |
| 2.5.3 | Differential Guiding | 19 |
| 2.5.4 | Image Analysis with OmegaCAM | 19 |
| 2.6 | Calibration lamps | 19 |
| 2.7 | Photometric Properties | 20 |
| 2.8 | Astrometric Properties | 20 |
| 3 | Observing with OmegaCAM | 21 |
| 3.1 | Offsetting Modes and Observing Strategies | 21 |
| 3.1.1 | Offsetting Modes | 21 |
| 3.1.2 | Observing Strategies | 22 |
| 3.2 | Atmospheric Refraction and Dispersion | 22 |
| 3.2.1 | Atmospheric Refraction | 22 |
| 3.2.2 | Atmospheric Dispersion | 23 |
| 3.3 | OB preparation | 24 |

| | | |
|----------|--|-----------|
| 3.3.1 | Target acquisition | 24 |
| 3.3.2 | Scientific exposure | 25 |
| 3.3.3 | Dither and jitter patterns | 25 |
| 3.4 | The Observing templates | 25 |
| 3.4.1 | Target Acquisition Templates | 25 |
| 3.4.2 | Science Templates | 25 |
| 3.4.3 | Nighttime Calibration | 26 |
| 3.4.4 | Overheads | 26 |
| 3.5 | Survey Area Definition Tool | 27 |
| 3.6 | Selecting exposure times and number of sub-exposures | 27 |
| 3.7 | Special features of the data | 27 |
| 3.7.1 | Point Spread Function | 27 |
| 3.7.2 | CCD blemishes and particle hits | 28 |
| 3.7.3 | Ghosts and reflections | 28 |
| 3.7.4 | Sky concentration | 29 |
| 3.7.5 | Diffraction Spikes | 29 |
| 3.7.6 | Fringes | 29 |
| 3.7.7 | Remanence | 31 |
| 3.7.8 | CCD Crosstalk | 31 |
| 4 | Calibrating and Reducing OmegaCAM data | 33 |
| 4.1 | Calibration Plan | 33 |
| 4.2 | Data reduction Pipeline | 35 |
| 4.3 | Quality Control | 35 |
| A | Filter throughput curves | 36 |
| A.1 | Broad band Sloan filters (ugriz) | 36 |
| A.2 | Segmented Broad-band filters (Johnson B and V) | 42 |
| A.3 | Narrow-band filters (Strömgren v and $H\alpha$) | 42 |
| A.4 | Radial variations in bandpass | 43 |
| B | Layout of the CCDs in the mosaic | 44 |
| C | Detector response curves | 45 |

List of Tables

| | | |
|---|--|----|
| 1 | Basic CCD characteristics | 9 |
| 2 | Filters available in OmegaCAM | 16 |
| 3 | OmegaCAM Photometric Standard Star Fields | 16 |
| 4 | Current OmegaCAM filter distribution. The opaque filter is required to protect the instrument when it is not in operation. | 17 |
| 5 | Magnitude zero points for the SDSS filter set. | 20 |
| 6 | Key difference between the dither and jitter modes. | 22 |
| 7 | Maximum airmasses without using the ADC | 24 |
| 8 | Overhead times for observations | 27 |

List of Figures

| | | |
|----|--|----|
| 1 | Schematic drawing of OmegaCAM | 3 |
| 2 | Optical layout of the VST | 4 |
| 3 | Spot Diagrams | 5 |
| 4 | Layout of the CCDs in the focal plane | 7 |
| 5 | Photograph of the detector mosaic | 8 |
| 6 | Single CCD pixel layout | 10 |
| 7 | Schematic of CCD readout | 11 |
| 8 | Linearity of the CCDs | 12 |
| 9 | Filter times CCD throughput | 13 |
| 10 | An OmegaCAM filter | 14 |
| 11 | Shadow cast by the cross in composite filters | 15 |
| 12 | Orientation of filter as function of magazine | 15 |
| 13 | The shutter unit | 18 |
| 14 | Limit on exposure time due to atmospheric refraction | 23 |
| 15 | OmegaCAM PSF anisotropies | 28 |
| 16 | Example ghost reflection | 30 |
| 17 | Reflection from a star outside the field | 31 |
| 18 | Crosstalk between CCDs 93–96 | 32 |
| 19 | Frequency of calibration observations | 34 |
| 20 | Filter measurement location and coordinate system | 36 |

21 *u* filter throughput 37

22 *g* filter throughput 38

23 *r* filter throughput 39

24 *i* filter throughput 40

25 *z* filter throughput 41

26 Technical drawing of CCD layout 44

27 CCD Quantum efficiency curves 45

1 Introduction

1.1 Scope

OmegaCAM is the wide-field imager for the Cassegrain focus of the VLT Survey Telescope (VST) on Paranal, a 2.6m modified Ritchie-Chretien alt-az telescope designed specifically for wide-field imaging. It is the only instrument on this telescope, and is operated most nights. In principle all observations are carried out in service mode. Its main function is to perform large optical imaging surveys, which may be used to feed the VLT telescopes with targets. With its wide field, broad-band filter set, and image quality matched to Paranal seeing conditions, OmegaCAM is well-suited to this task.

This document serves as a user manual for those planning or preparing observations with OmegaCAM. It describes the main instrument characteristics, and how to observe with it using Observation Blocks and Observing Templates.

1.2 More Info

Further information can be obtained by contacting usd-help@eso.org.

1.3 References

[RD1] Template Manual, VST-MAN-OCM-23100-3111,
see <http://www.eso.org/sci/facilities/paranal/instruments/omegacam/doc/>.

[RD2] Calibration Plan, VST-PLA-OCM-23100-3090,
see <http://www.eso.org/sci/facilities/paranal/instruments/omegacam/doc/>.

[RD3] DFS User Requirements, VST-SPE-OCM-23100-3050,
see <http://www.eso.org/sci/facilities/paranal/instruments/omegacam/doc/>.

[RD4] WFI documentation, see <http://www.ls.eso.org/lasilla/sciops/2p2/E2p2M/WFI/>.

[RD5] P2PP instructions, see <http://www.eso.org/sci/observing/phase2/P2PPSurveys.html/>.

1.4 Acronyms

ADC: Atmospheric dispersion compensator, a device which corrects for the chromatic effects of the atmosphere at low elevations.

CCD: Charge-couple device, a solid-state, panoramic light detector of high quantum efficiency.

DFS: Data Flow System.

e2v: Manufacturer of the OmegaCAM CCDs.

ETC: Exposure Time Calculator, a software tool provided by ESO as an aid in planning observations.

FWHM: Full Width at Half-Maximum.

MPG: Max Planck Gesellschaft.

OB: Observation Block, a set of instructions to telescope and instrument to carry out a specific observation.

OmegaCAM: The wide-field CCD camera for the VST.

P2PP: Phase 2 Proposal Preparation, the process at ESO in which the users define the OBs for their approved programmes by means of special software.

PA: Position Angle, orientation of the field of view on the sky.

RMS: Root-mean square.

SADT: Survey Area Definition Tool

SDSS: Sloan Digital Sky Survey, a large imaging and spectroscopy survey of (mostly) the Northern hemisphere. OmegaCAM's science filter set include the five SDSS filters $u'g'r'i'z'$.

USNO: US Naval Observatory. Their all-sky catalogue is used for astrometric calibration of OmegaCAM data.

VLT: Very Large Telescope, four 8m telescopes on ESO's Paranal Observatory.

VST: VLT Survey Telescope, a 2.6m telescope at ESO's Paranal Observatory dedicated to optical surveys, and host to OmegaCAM.

WFI: Wide-Field Imager, an 8-CCD mosaic camera on the ESO/MPG 2.2 telescope on La Silla with similar pixel scale and sensitivity to OmegaCAM.

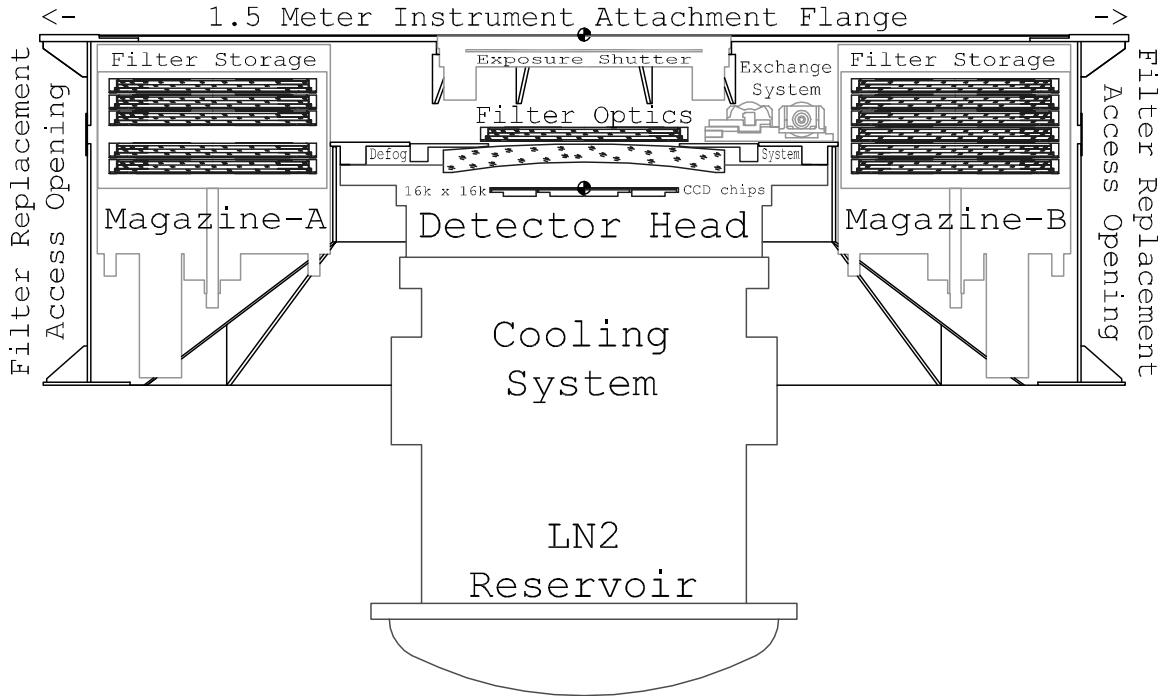


Figure 1: Schematic view of the instrument. Key components are labelled.

2 Instrument characteristics

2.1 Overview

OmegaCAM (see Fig. 1) is the wide-field imager for the Cassegrain focus of the VLT Survey Telescope (VST) on Paranal, a 2.6m modified Ritchie-Chretien alt-az telescope designed specifically for wide-field imaging. It is the only instrument on this telescope, and is operated most nights. In principle all observations are carried out in service mode.

The VST/OmegaCAM system is designed for good seeing-limited image quality over a wide field. The telescope has an actively controlled meniscus primary mirror, an active secondary, and an image analysis system. It contains two interchangeable correctors: one is a high-throughput two-lens corrector which works in u-z bands, the other contains an Atmospheric Dispersion Compensator (ADC) for work at lower elevations. The ADC has no throughput in the u band.

The optical layout of the VST is illustrated in Fig. 2.

The VST provides a 1 degree unvignetted field of view, which OmegaCAM samples with a 32-CCD, 16k x 16k detector mosaic (Fig. 4) at 0.21 arcsec per pixel (0.2134 for the two-lens corrector, 0.215 for the ADC configuration). The CCDs are thinned, blue-sensitive, 3-edge buttable CCD44-82 devices from e2v of high (but not perfect) cosmetic quality. Image quality is specified such that in the absence of seeing 80% of the energy from a point source should fall within a 2x2 pixel area over the full field (see example spot diagrams in Fig 3). The field distortion is very low, so that the image scale is virtually constant over the whole field. There are narrow gaps between the CCDs: the overall geometric filling factor of the array is 91.4%.

In addition to the 32 CCDs making up the science array, OmegaCAM also contains four auxiliary CCDs around the edges of the field. Two of these are used for autoguiding, so that both field position and rotation can be tracked accurately. The other two auxiliary CCDs are mounted 2mm outside the

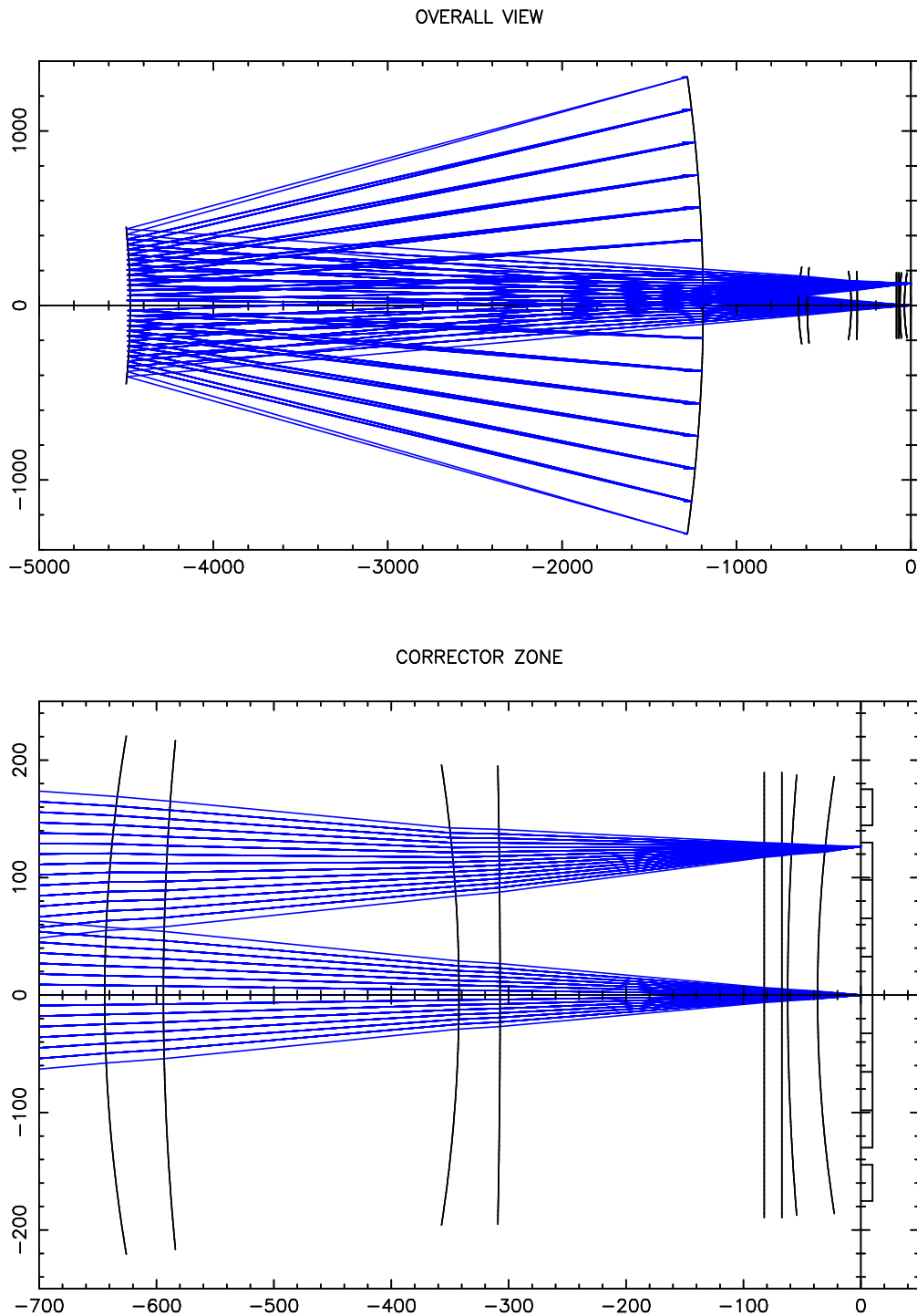


Figure 2: Optical layout and selected light paths through the VST. The configuration with the two-lens corrector is shown. The bottom panel shows a zoom onto the corrector optics: the incoming light passes through two spherical lenses, a planar filter, and the spherical dewar entrance window before striking the CCDs on the right. Scales are in mm.

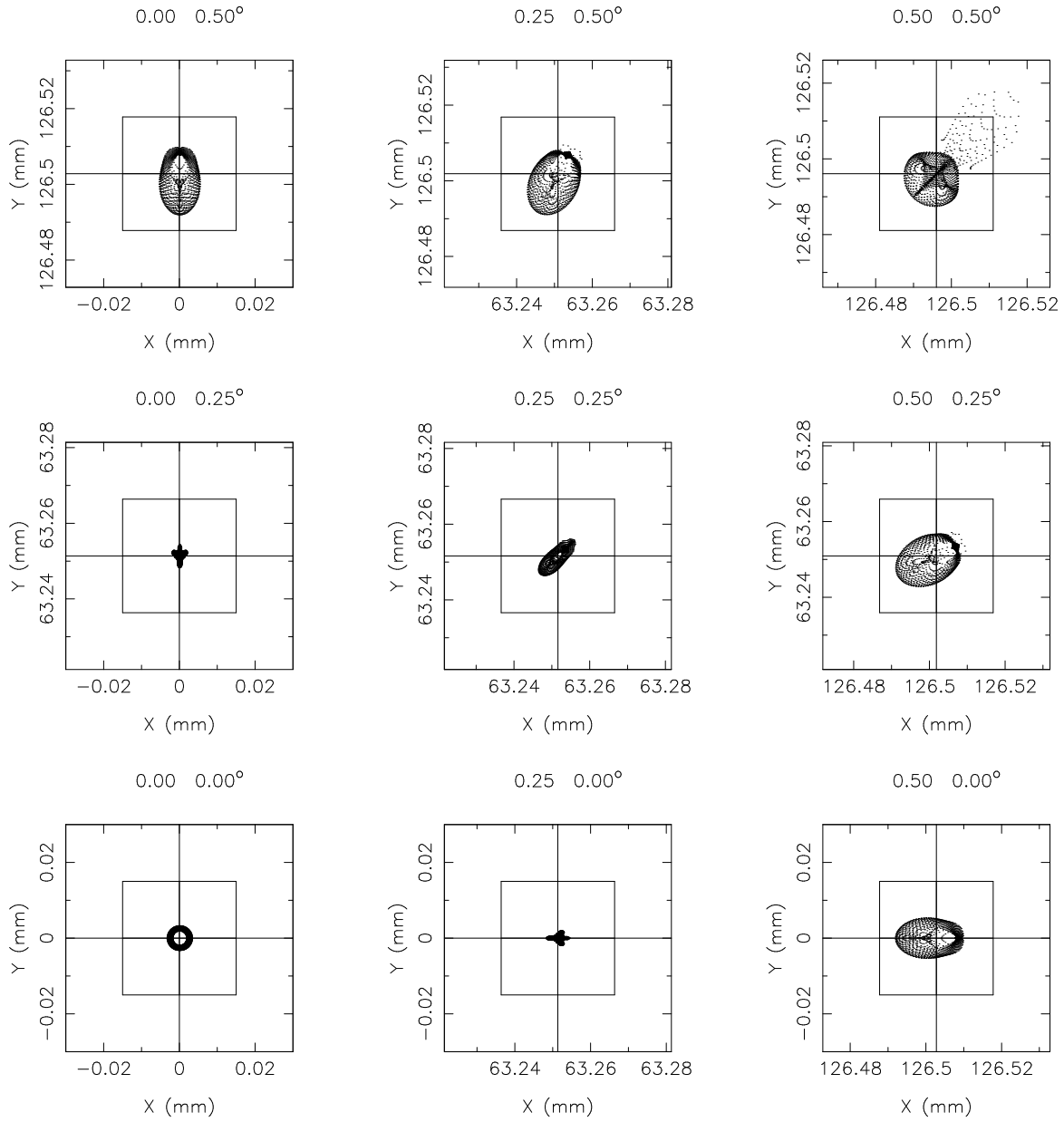


Figure 3: Sample spot diagrams for 500nm light in a quadrant of the OmegaCAM focal plane. A 2x2 pixel grid ($30\mu\text{m} \times 30\mu\text{m}$, corresponding to $0.43''$) is shown as well.

focal plane (one in front, one behind), and are used for recording defocused star images for on-line analysis of the image quality. The CCD layout in the focal plane is shown in Fig. 4 and in more detail in Appendix B. A photograph of the detector mosaic is shown in Fig. 5.

OmegaCAM contains a 12-filter exchange mechanism. Currently the available filters include the Sloan $u'g'r'i'z'$ set, Johnson B and V filters, several narrow-band filter mosaics, a Strömberg v filter, and a special calibration filter (see Table 2).

OmegaCAM data are taken in the context of a calibration plan [RD2] that ensures that all data can be photometrically and astrometrically calibrated to 0.05 magnitudes and 0.1 arcsec rms precision, respectively.

Compared to the wide-field imager (WFI [RD4]) on the ESO/MPG La Silla 2.2m telescope, OmegaCAM on the VST offers

1. a four times larger field
2. better cosmetic quality CCDs
3. a primary mirror of 1.4 times the area
4. year-round operation in service mode
5. better image quality due to active telescope optics, astro-climate, ADC
6. a data flow pipeline for automatic reduction of data
7. the Sloan filter set

2.2 Detector Mosaic

2.2.1 The 268-Million Pixel Science Array

The central 32 CCDs of OmegaCAM form the science array, the heart of the instrument. Basic characteristics of the CCDs are found in Table 1.

The packaging of a single CCD is illustrated in Fig. 6. The light-sensitive area consists of 4100x2048 pixels, surrounded by a border whose width is 0.16mm on the short side opposite the readout register, 0.5mm along the long sides of the CCD, and 5mm on the side of the readout register. Unavoidably therefore, there are small 'dead zone' gaps in the science array between the light-sensitive areas of neighbouring CCDs. How the CCDs are mounted together in the array is indicated in Figs. 4 and 5 above. All CCDs are read out at 280kpix/s, through one amplifier/port. The resulting image comes with 48 columns of pre- and overscan, and 100 rows of vertical overscan. Because of their construction and the way they are arranged in the mosaic, all CCDs are read out along their long side, in a direction away from the center of the mosaic.

The readout sequence is illustrated in Fig. 7. The science mosaic is read out by two FIERA systems, one for each half of the array. Total readout time is 29sec. Combined with other overheads, principally the time needed to wipe the array before a new exposure, this leads to a total minimum shutter-closed time between successive exposures of 40 seconds.

Generally the CCDs in the array are similar, but they do differ in detail. Below a number of properties of the CCDs are tabulated, in a format that corresponds to their layout in the science array. At the default sky position angle of zero degrees this layout corresponds to N at the top, and East to the *right*.

Complete QE curves for each of the CCDs are given in Appendix C.

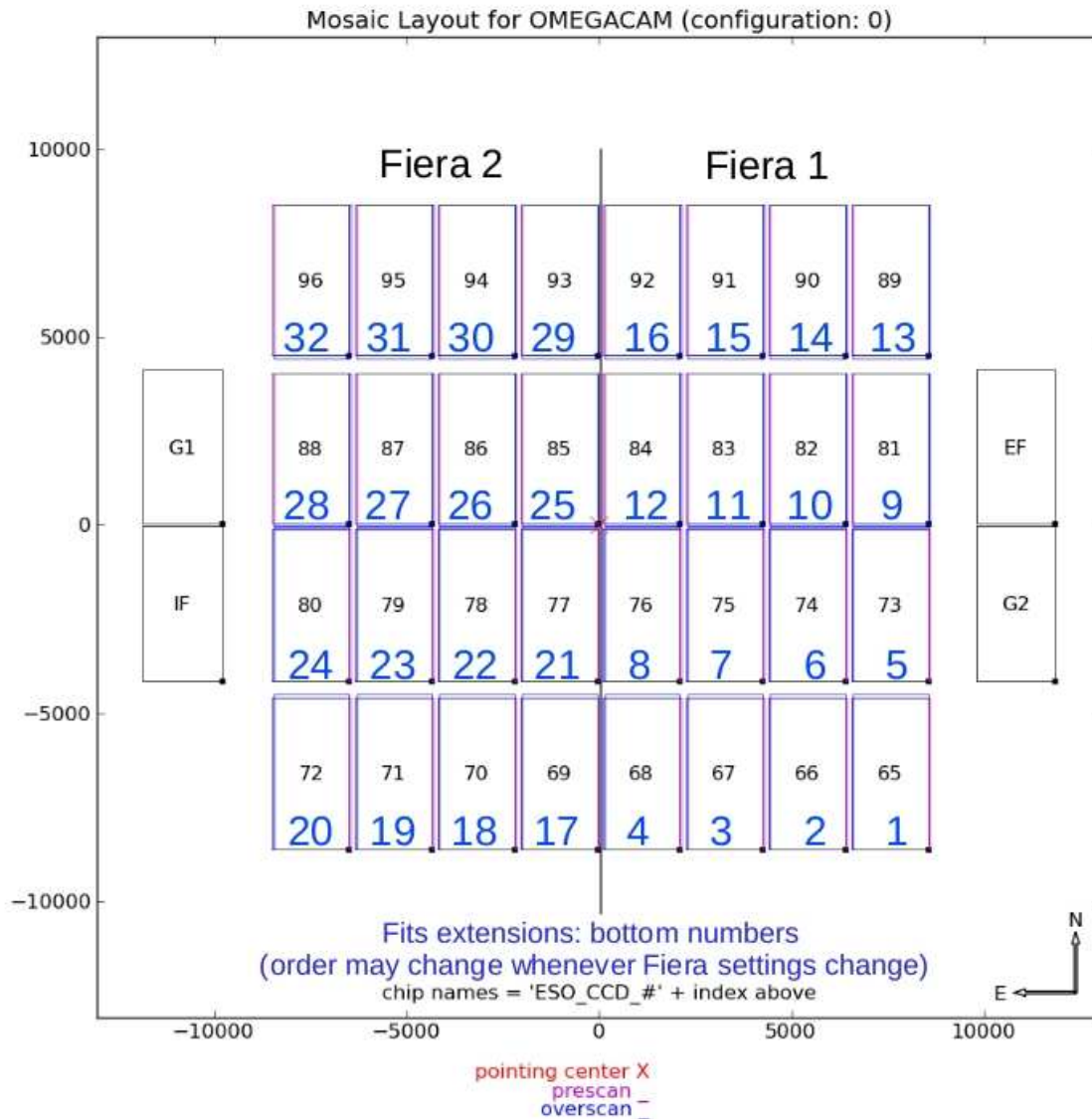


Figure 4: The layout of the 32 science CCDs and the four auxiliary CCDs in the focal plane. The science array covers a 1 degree x 1 degree area of sky, with 16k x 16k pixels of 0.21 arcsec. All CCDs fit inside a circle of diameter 1.4 degrees on the sky. (Note that this is the layout as seen from below, i.e., the projection of the array onto the sky.)

OmegaCAM data are delivered as multi-extension FITS files. The CCD name (#65–96) is included in the header of each fits extension. CCDs can also be identified by the number of their fits extension, but beware: this order may change from what is shown in the Figure whenever CCD controller parameters are changed.

Two of the auxiliary CCDs are mounted out of the focal plane (IF & EF), at displacements ± 2 mm, in order to enable image analysis and real-time active optics corrections. G1 and G2 are used for guiding.

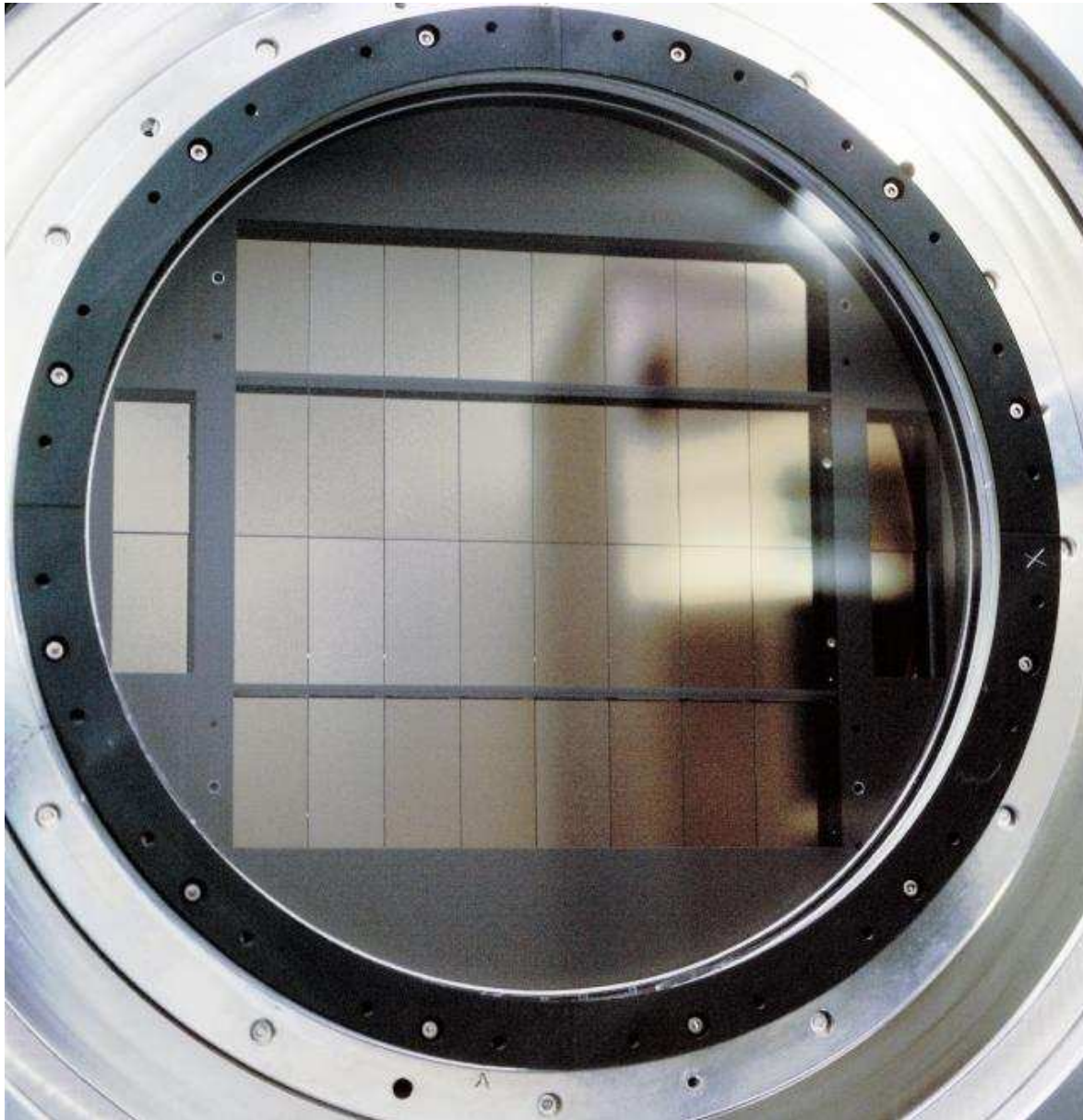


Figure 5: Picture of the 36 CCDs mounted behind the dewar window. Note the black strips that cover the gaps between the CCDs: they prevent reflection of light off the bright bond wires of each detector. Slight vignetting is observed near these strips, and on the long outer sides of the four corner CCDs.

| CCD Parameter | Value |
|-------------------------------------|---|
| CCD type | Marconi / e2v / CCD 44 - 82 - 1 - A57 thin devices (20 μ m) |
| Pixel size | 15 μ m |
| Format | Active Pixel Area 2048 x 4102 pixels (2048x4100 used) 50 horizontal pre- and 50 overscan pixels |
| Flatness | < 20 μ m peak to valley |
| R.O.N. (not including system noise) | 2 e ⁻ at 50 kpix/sec 4 e ⁻ at 500 kpix/sec 6 e ⁻ at 1000 kpix/sec |
| Output Amplifiers | 2 identical output amplifiers with integrated post chip amplifiers. Charge can be read through either one completely or through both of them simultaneously |
| Device Layout | No frame transfer option, 3 phase parallel register (non split), 3 phase serial register (split) |
| Dump Drain | A dump drain exists parallel to the serial readout register, so that lines can be discarded as a whole |
| Cosmetics | A global defect budget exists, specifying the overall defects for all of the 40 science devices (Cosmetically the final device cosmetics are much better than devices used for the WFI) |
| CTE | > 0.999995 per parallel or serial shift |
| Horizontal Transfer Frequency | 2 Mpixels/sec |
| Vertical Transfer Frequency | 15-20 klines/sec |
| Full Well / Linearity | >200 000 e ⁻ . Serial full well is at least 2 times the pixel full well and the summing full well is at least 4 times the pixel full well. These full well values correspond to the maximum charge that can be handled while attaining the CTE specified. Amplifier full well is around 200 000 e ⁻ . Amplifier full well refers to the limit of linearity, i.e. the maximum amount of charge that can be amplified while producing output that matches a linear response to within 1 %. |
| Dark Current | < 2 e ⁻ / pixel / hour (at operating temperature of -120 °C) |
| Cosmic Ray Sensitivity | < 3 events / square cm and minute |
| Optical Coating | Single layer anti reflection coating astro BB (with thickness 42nm instead of 46nm) |
| Package design | Four side buttable (fourth side with larger gap), Invar package with integrated PT100 temperature sensor |

Table 1: Basic characteristics of the OmegaCAM CCDs

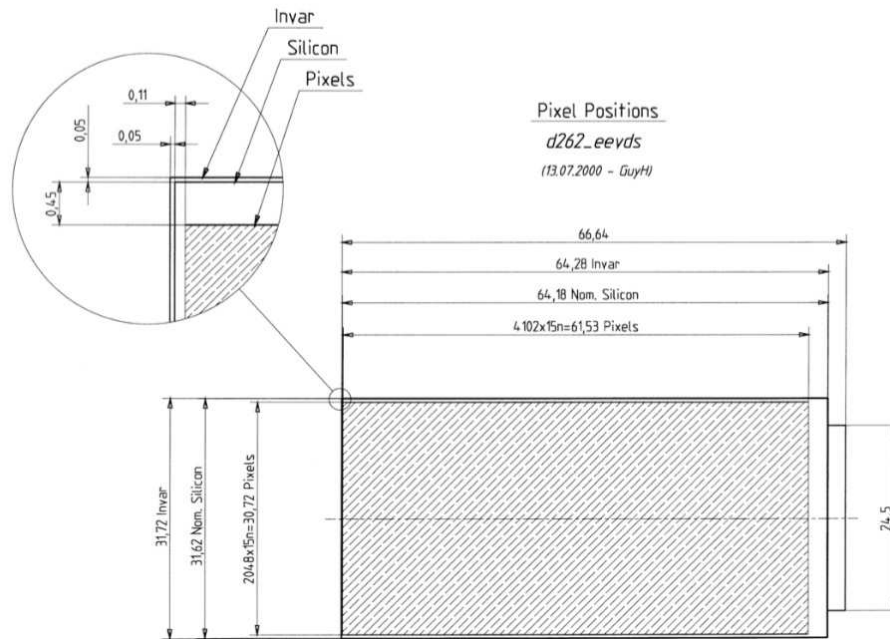


Figure 6: The light-sensitive area of a single CCD.

N (at PA 0 degrees)

| |
|-----------------------|
| CCD number |
| gain (e-/ADU) |
| readnoise (e-) |
| # hot pixels |
| # cold pixels |
| dark current (ADU/hr) |

| | | | | | | | |
|------|-------|------|------|------|-------|-------|------|
| #89 | #90 | #91 | #92 | #93 | #94 | #95 | #96 |
| 2.37 | 2.52 | 2.62 | 2.56 | 2.56 | 2.78 | 2.73 | 2.37 |
| 6.52 | 6.23 | 5.98 | 6.03 | 5.15 | 5.61 | 6.90 | 5.17 |
| 50 | 14 | 11 | 24 | 18 | 16 | 17 | 18 |
| 3143 | 16719 | 8891 | 4926 | 7037 | 15038 | 10134 | 7222 |
| 0.50 | 0.46 | 0.36 | 0.47 | 0.27 | 0.37 | 0.15 | 0.34 |
| #81 | #82 | #83 | #84 | #85 | #86 | #87 | #88 |
| 2.57 | 2.56 | 2.56 | 2.46 | 2.40 | 2.32 | 2.39 | 2.52 |
| 5.20 | 5.05 | 5.22 | 5.06 | 5.19 | 4.82 | 5.10 | 5.22 |
| 25 | 3490 | 28 | 825 | 11 | 13 | 19 | 9 |
| 8698 | 2816 | 9611 | 5713 | 9742 | 6420 | 8570 | 9553 |
| 0.36 | 0.28 | 0.41 | 0.31 | 0.33 | 0.40 | 0.37 | 0.38 |
| #73 | #74 | #75 | #76 | #77 | #78 | #79 | #80 |
| 2.40 | 2.48 | 2.52 | 2.44 | 2.66 | 2.71 | 2.67 | 2.57 |
| 4.70 | 5.18 | 5.12 | 4.97 | 5.95 | 5.31 | 5.36 | 5.17 |
| 7 | 16 | 18 | 20 | 13 | 7 | 58 | 50 |
| 3811 | 2692 | 2765 | 2802 | 2683 | 2660 | 2911 | 4329 |
| 0.35 | 0.22 | 0.21 | 0.28 | 0.33 | 0.26 | 0.24 | 0.29 |
| #65 | #66 | #67 | #68 | #69 | #70 | #71 | #72 |
| 2.39 | 2.59 | 2.49 | 2.55 | 2.48 | 2.23 | 2.54 | 2.39 |
| 4.73 | 5.10 | 5.20 | 5.42 | 5.28 | 4.69 | 5.08 | 4.83 |
| 7 | 131 | 25 | 109 | 18 | 20 | 16 | 13 |
| 2807 | 5363 | 2956 | 4163 | 3003 | 5783 | 7371 | 4191 |
| 0.30 | 0.36 | 0.26 | 0.30 | 0.25 | 0.31 | 0.27 | 0.28 |

E

All CCDs but three have parallel and serial cte above 0.999995, the exceptions being:

- CCD #65 and #96, which have serial cte 0.999994
- CCD #72 which has serial cte 0.999993

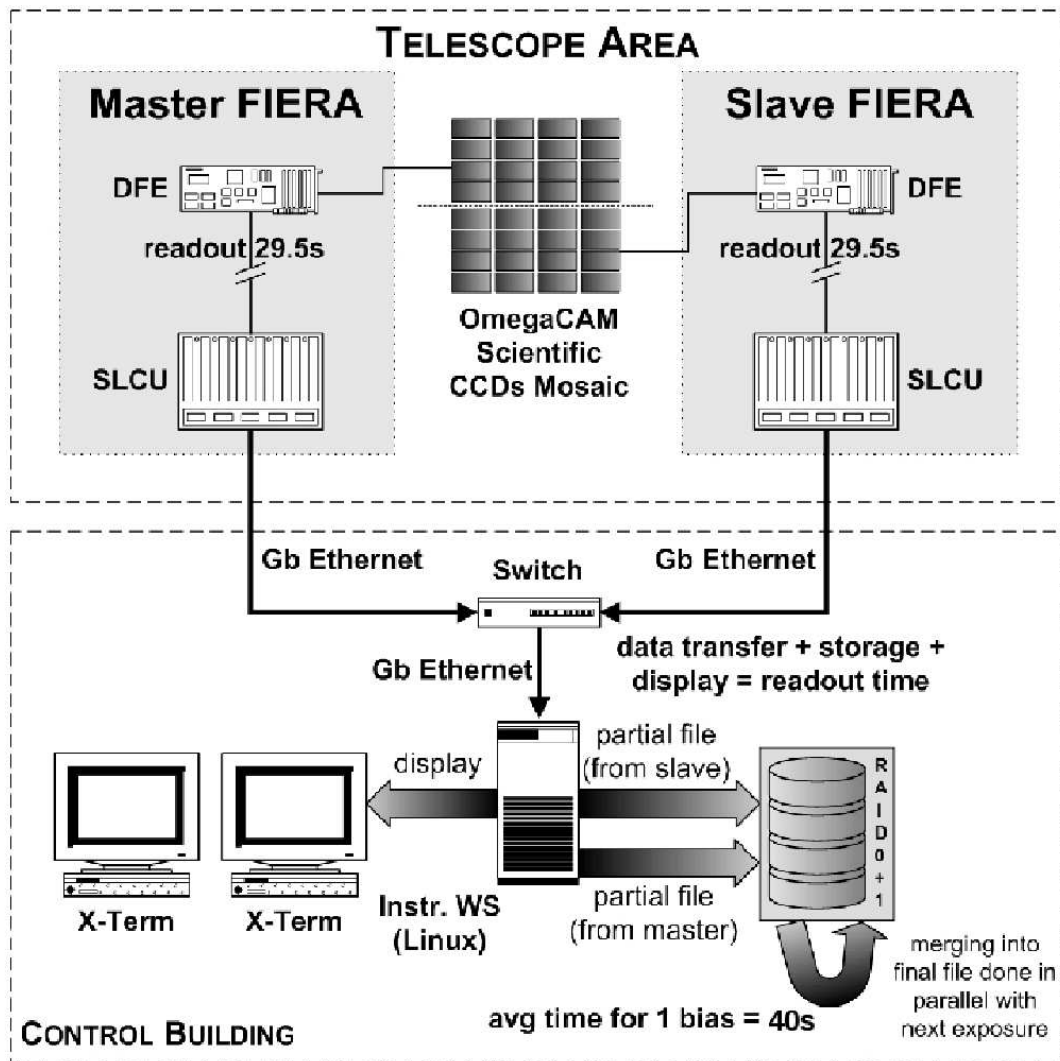


Figure 7: Data flow diagram for readout of the OmegaCAM science array.

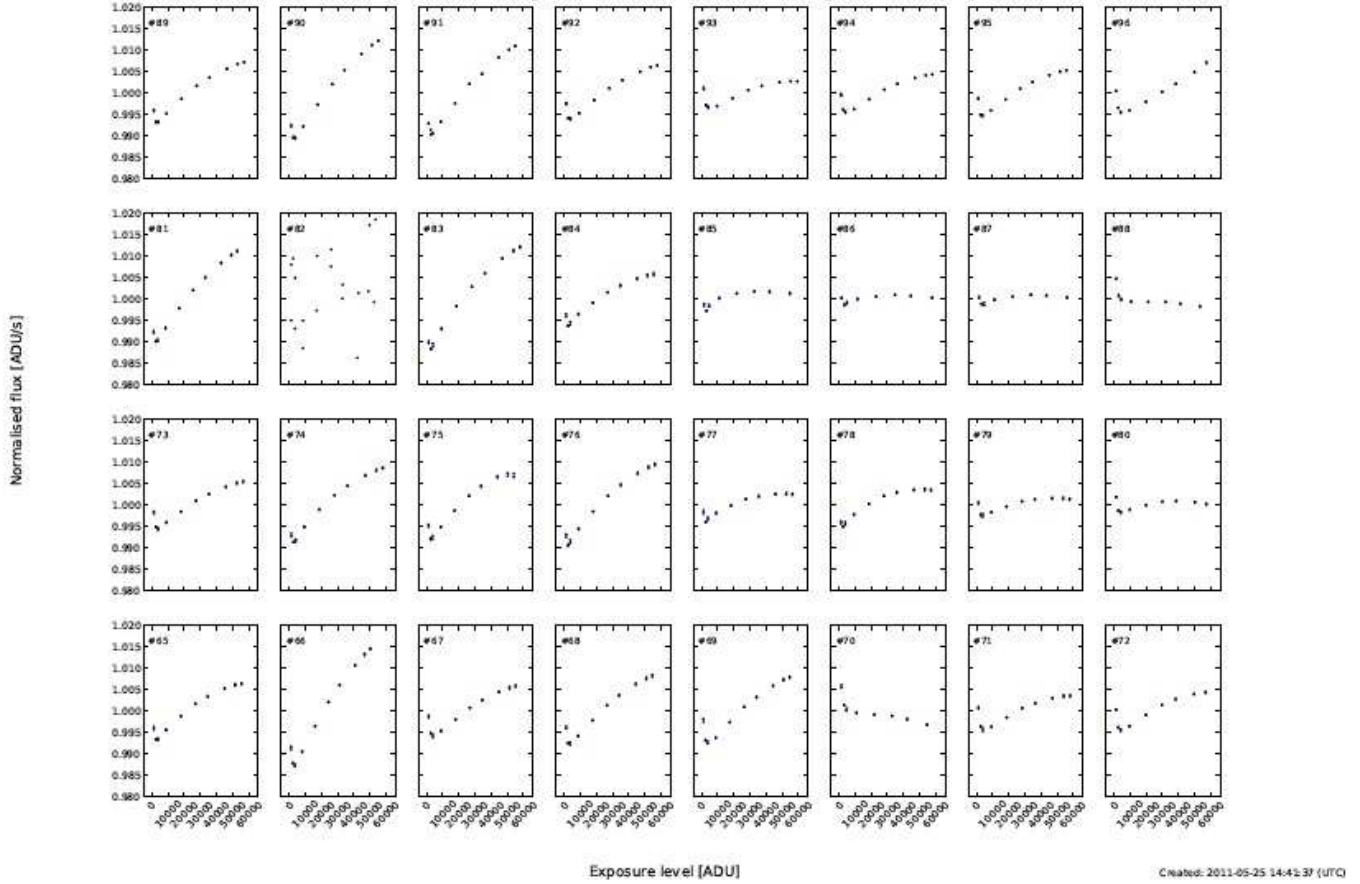


Figure 8: Plot of the linearity of the response of each CCD, as a function of illumination level. (Obtained by exposing the mosaic to a calibration lamp, with varying exposure times).

With a gain of ca. 2.5 electrons per ADU, the analog-to-digital conversion of the amplifier output of each CCD saturates before the CCD full-well capacity of over 200,000 electrons. Below this saturation the response of the CCDs is linear to within 1%, as can be seen from Fig. 8.

The flat fields of the CCDs show different behaviour, dependent on the wavelength. In the u band, the flat fields show a diagonal, diamond-like pattern, which is caused by the thinning process. A few of the CCDs (#65, 66, 86, 87) also show an 'ink pattern', areas of very high UV sensitivity (the origin of this feature is unknown). At intermediate wavelengths (g , r) the flat fields are reasonably featureless. At longer wavelengths (i and particularly z), fringing occurs, leading to swirling patterns reminiscent of a thin film of oil on water. All artifacts can be removed in data reduction.

The efficiency of the filters, folded with the detector response, is plotted in Fig. 9. Detailed analysis of the filter throughput, including bandpass variations across the fields, are deferred to Appendix A.

See §3.7 for a description of particular features that occur in scientific data obtained with OmegaCAM, many of which follow from the properties of the detectors.

2.2.2 Auxiliary CCDs

In the periphery of the focal plane OmegaCAM contains four auxiliary CCDs. Two of these are used for guiding, both in position and position angle of the field. The other two are mounted out of focus

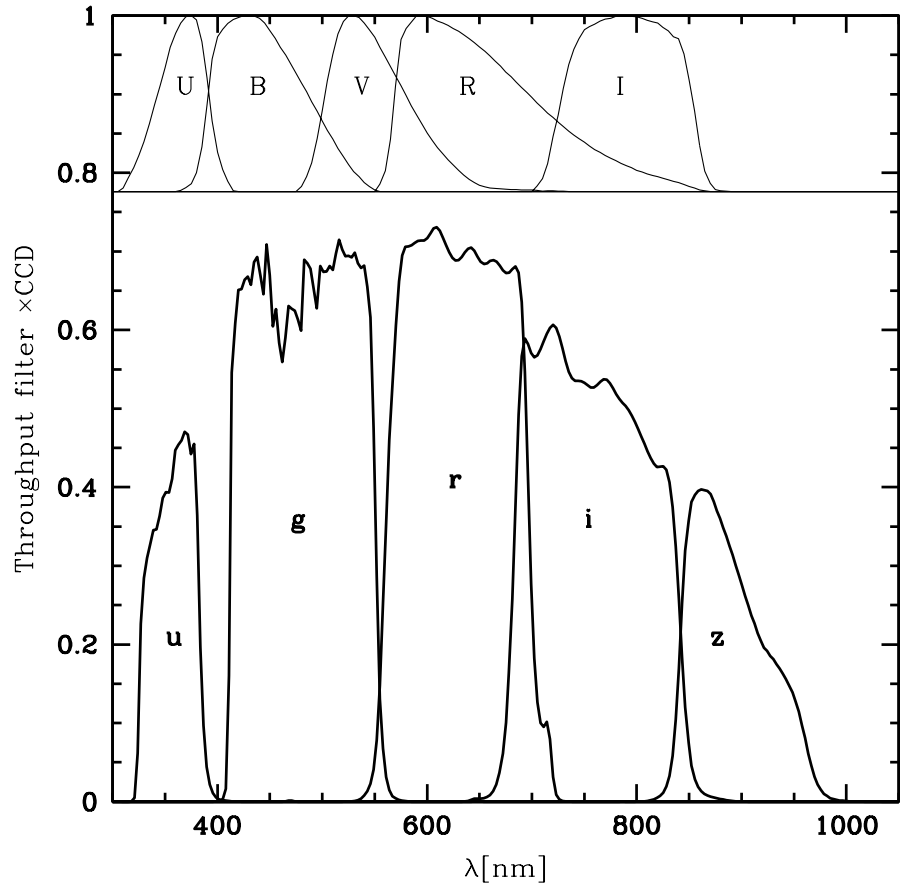


Figure 9: Throughput of the OmegaCAM Sloan filters, times the average quantum efficiency of the CCDs. For comparison the standard Johnson-Cousins UBVRI filters are also shown.

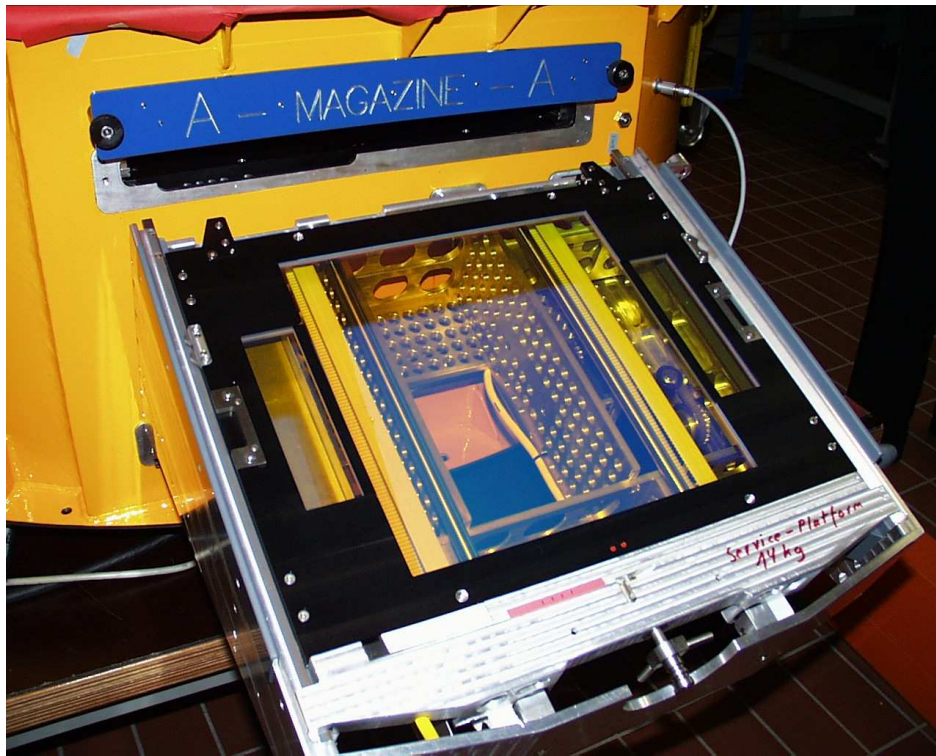


Figure 10: A single OmegaCAM filter ready to be loaded into the instrument. Note the separate filters covering the auxiliary CCDs.

(one is 2mm in front of the focal plane, one 2mm behind). Analysis of pairs of defocused images from these CCDs allows optical aberrations (defocus, coma, astigmatism, ...) to be measured and the telescope to be kept in focus.

2.3 Filters

The filter exchange mechanism (Fig. 10) selects filters from two magazines located either side of the focal plane inside the instrument, and slides these into the beam. Each magazine can store six filters. Filter positioning is repeatable to very high accuracy resulting in less than 0.3% rms flux variations between flat fields taken at different times. The footprint of a stellar image is about 1cm in size.

The available filters are listed in Table 2. Transmission curves as measured in the lab are included in Appendix A.

The filters are sandwiches of glass substrates, ca. 14mm thick. Each filter has a baseplate (usually made of BK7) which provides the mechanical support and mounting to the filter frame. Further layers of glass are glued onto this base plate, and provide the filter bandpass, either through coating or by means of coloured glass. In some cases (the ‘segmented’ filters) these layers consist of four quadrants, and the interface of the quadrants casts a slight shadow in the form of a cross onto the image plane (Fig. 11). Most of the narrow-band filters consist of quadrants where each quadrant has a different bandpass. By offsetting the telescope in half-degree steps, and/or rotating the instrument through multiples of 90 degrees, the full field of view can be exposed in all four bandpasses. Which CCD was exposed with which filter segment depends on the magazine the filter is loaded in - this is recorded in the image FITS header (see below, Note on filter magazines).

The auxiliary CCDs, used for guiding and image analysis, are covered by separate filters. Usually these have nearly the same bandpass as the main science filter, but in some cases (the narrow band

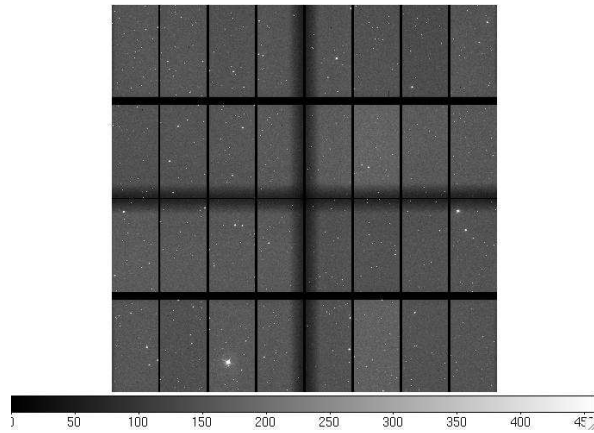


Figure 11: The shadow cast by the cross that separates the different segments of a composite filter (here the V filter).

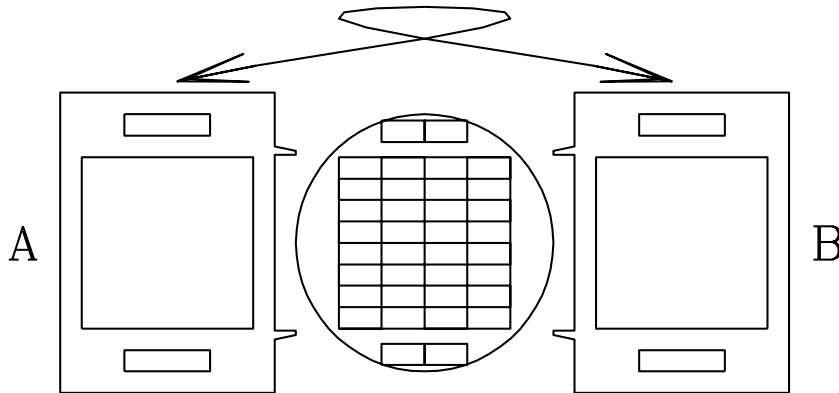


Figure 12: Orientation of a filter depends on whether it is loaded in magazine A or B.

filters and the u band filter) they are different, in order to boost sensitivity and increase the number of guide stars that can be used.

Filter exchange time varies from 65 to 115 seconds, depending on how far the magazines need to move, and on whether the incoming and outgoing filters belong in the same magazine (which gives the longer exchange time) or not.

The Calibration filter is used to observe standard star fields in four bands simultaneously, and hence to monitor variations in the atmospheric extinction throughout the night. For this purpose specially calibrated standard star fields (Landoldt fields, extended to a square degree) have been established around the celestial equator, and near the South celestial pole. They are listed in Table 3. The full calibration of these extended fields is ongoing during the first year of operations.

2.3.1 Note on filter magazines

Because the filter frames can only mate with the filter insertion mechanism on one side, the orientation of a filter with respect to the CCD mosaic depends on the magazine in which it was stored (see Fig. 12). During observations the filter exchange mechanism always returns a filter to the magazine (and slot within that magazine) it came from. However, it may happen that a filter needs to be moved manually from one magazine to the other during daytime operations. This flips the orientation of the filter by

Table 2: Filters available in OmegaCAM

| Filter name | System | λ (nm) ^a | $\Delta\lambda$ (nm) ^b | P2PP name | comment ^c |
|----------------------|-----------|-----------------------------|-----------------------------------|--------------------|----------------------|
| u' | SDSS | 354 | 56 | u_SDSS | IF, M |
| g' | SDSS | 475 | 134 | g_SDSS | IF, M |
| r' | SDSS | 625 | 135 | r_SDSS | IF, M |
| i' | SDSS | 756 | 155 | i_SDSS | IF, M |
| z' | SDSS | 880 | 80 | z_SDSS | IF, M |
| B | Johnson | 439 | 103 | B_JOHN | IF, S |
| V | Johnson | 551 | 98 | V_JOHN | IF, S |
| v | Strömgren | 412 | 21 | v_STRM | IF, M |
| $H\alpha^d$ VPHAS+ | — | 658.6, 659.3 | 10.5 | NB_659 | IF, S |
| $H\alpha^e$ | — | 659.0, 666.0, 672.6, 679.1 | 11 | H_ALPHA | IF, 4Q |
| $H\alpha(z = 0.3)^f$ | — | 851.9, 861.4, 869.0, 877.7 | 12.5 | NB_852_861_869_878 | IF, CG, 4Q |
| NB3 ^f | — | 453.6, 494.3, 533.5, 575.6 | 15–20 | NB_454_494_533_575 | IF, CG, 4Q |
| NB4 ^f | — | 616.1, 710.2, 755.1, 816.4 | 13–20 | NB_617_710_755_817 | IF, CG, 4Q |
| Calib ^g | SDSS | u', g', r', i' | | u_g_r_i_SDSS | IF, CG, 4Q |

^aCentral wavelength and ^bFWHM of filter throughput \times mean CCD QE curve

^cIF=Interference Filter; CG=Coloured Glass filter; M=Monolithic; S=Segmented; 4Q=4 quadrants with different passband.

^dThis is a private filter for the VPHAS+ survey. Note the slightly different central wavelength of one of the segments.

^e $H\alpha$ in four slightly overlapping redshift ranges: $z = 0, 0.01, 0.02, 0.03$.

^fThese are private filters for use by Munich University Observatory for the first five years of OmegaCAM operations. **Note that these are not mounted at present.**

^gBecause of the different manufacturing processes, the Calib filter bandpasses differ in detail from the monolithic filters.

For the filters consisting of different quadrants, the layout of the quadrants on the sky is as shown below when the filter is inserted in magazine A (for the default orientation of the instrument with PA=0, North is up, East to the left). If the filter is mounted in magazine B the orientation is rotated by 180 degrees.

| $H\alpha$ | | $H\alpha$ VPHAS+ | | $H\alpha(z = 0.3)$ | | NB3 | | NB4 | | Calib | |
|-----------|-----|------------------|-------|--------------------|-----|-----|-----|-----|-----|-------|------|
| 679 | 673 | 658.6 | 658.6 | 852 | 869 | 494 | 454 | 710 | 616 | u' | i' |
| 659 | 666 | 659.3 | 658.6 | 861 | 878 | 533 | 576 | 816 | 755 | g' | r' |

| Field Name | RA | DEC |
|-------------|------------|-------------|
| SA92 | 00:55:12.0 | 00:55:58.0 |
| SA95 | 03:53:49.0 | 00:02:33.0 |
| SA98 | 06:52:12.0 | -00:19:17.0 |
| SA101 | 09:56:19.0 | -00:26:27.0 |
| SA104 | 12:42:12.0 | -00:30:16.0 |
| SA107 | 15:39:03.0 | -00:13:52.0 |
| SA110 | 18:41:50.0 | 00:23:09.0 |
| SA113 | 21:41:54.0 | 00:29:22.0 |
| Polar Field | 03:25:43.0 | -89:02:33.0 |

Table 3: OmegaCAM Photometric Standard Star Fields

| Magazine A | Magazine B |
|------------|------------|
| u | opaque |
| r | g |
| z | i |
| V | B |
| v | Halp |
| calib | NB659 |

Table 4: Current OmegaCAM filter distribution. The opaque filter is required to protect the instrument when it is not in operation.

180 degrees.

Manual filter manipulations should always be followed by the taking of a new set of flat fields, but if for some reason old flats need to be used it is important to check that these were taken with the same filter orientation. Which magazine a filter was loaded from is logged in the image headers (keyword INS.FILT1.NO: magazine ‘A’ contains filter positions 1–6; magazine ‘B’ positions 7–12).

The current order in which the filters are stored in the instrument is shown in Table 4

2.3.2 Providing Private Filters

It is possible, but not simple, to use private filters with OmegaCAM. There are a number of constraints:

1. The filters need to be mounted in special frames. These frames grab the filters by the baseplate, which needs to be approx. 5mm thick. Spare frames exist.
2. Overall optical thickness should be equivalent to 15mm fused silica.
3. The costs of these large filters are high (50-100 kEuro), and manufacturing times long (up to a year or more).

People interested in using private filters with OmegaCAM should contact the ESO User Support Department (usd-help@eso.org).

2.4 Shutter

The shutter of OmegaCAM is located on top of the instrument, in front of the filters. When closed it covers all 36 CCDs (science + auxiliary). It is a low-acceleration, twin-blade photometric shutter of aperture 370×292mm. The leading blade exposes the CCDs, the trailing blade covers them again. By ensuring that both blades travel with the same acceleration profile the exposure is kept homogeneous over the full beam. For very short exposures (below 0.8 s) the trailing blade starts its motion before the leading blade has finished moving. Over the science CCDs the blades move at constant speed.

Even for exposures as short as 0.1 seconds, the homogeneity over the field is better than 1%. However, it is important to realize that exposures are not simultaneous: there is a lag of about 0.5 second between the exposures at the leading and trailing edge of the field. For high timing accuracy observations, the delay time

$$t_{\text{delay}} = 0.39 + 0.00174X \text{ seconds} \quad (1)$$

needs to be added to the absolute time of the exposure start and end. Here, X is in mm with respect to the center of the detector mosaic (1mm=14.3 arcsec), and runs along the short sides of the CCDs in the direction of motion of the blades.



Figure 13: Picture of the partly disassembled shutter unit (Bonn shutter). The two blades, as well as the central aperture, are visible in the lower part of the unit.

The signs of the header keywords DET SHUT TMCLOS and DET SHUT TMOPEN record from which direction the shutter was opened.

Note that the shutter blades are quite far from focus: at the shutter location the light from a given star is smeared out over a width of about one tenth of the full shutter aperture. This means that the time over which a given pixel receives photons is longer than the actual exposure time, by an amount of roughly 0.08 s. Seen from an individual pixel the photon rate over time does not have steep edges but is smeared out.

2.5 Auto-Guiding and Focussing

Both the VST and OmegaCAM contain systems for auto-guiding and for focussing. Focussing happens automatically through real-time sensing of the wavefront. (Filter-dependent focus offsets are also automatically applied.) Traditional through-focus sequences are only needed to calibrate these auto-focus systems.

The VST tracks very well, and for exposures shorter than 60 sec there is no need to auto-guide. Depending on the user's image quality requirements, up to 2-3 minutes without guiding can be accepted. Commissioning and verification tests have shown that tracking drifts are of order $\sim 0.1\text{-}0.2''$ per minute, but can increase when the telescope approaches zenith. Whether autoguiding is desired or not can be specified in the acquisition template of an Observation Block.

2.5.1 VST Guide Probe

The VST contains a guide probe with a pick-off mirror, which can patrol the field in front of the filters. It can be used for guiding the telescope and for its active optics system. When required, the probe can be used in between scientific exposures to measure the optical image quality by means of a Shack-Hartmann analysis. This information can then be used to configure the telescope's active optics system.

The probe can in principle also be used for autoguiding and image analysis during scientific exposures. However, unless a suitable guide star exists very close to the edge of the field, the probe vignets the field of view. Use of the OmegaCAM guide and image analysis sensors is thus the default way of

operating OmegaCAM and VST. It also avoids the need to move the VST probe in and out of the field, which takes several minutes.

2.5.2 Auto-guiding with OmegaCAM

Two guider CCDs are mounted diametrically opposite to each other, near the edges of the field (see Fig. 4). Auto-guiding is done simultaneously on two stars, one on each guider CCD, or with a single star on one of the two chips. Guiding with two stars allows field center and rotation to be tracked during an exposure. When the shutter closes, the guider CCDs are not exposed to the sky, and guiding cannot take place. Acquisition of the two guide stars, one per CCD, happens automatically. If after a readout a second exposure is taken of the same field, the guide stars are re-acquired once the shutter is reopened. If there was no offset commanded for this new exposure, then the auto-guiding will attempt to return the guide stars to the same pixels as in the previous exposures. If an offset is commanded, the auto-guiding will simply keep the stars on the pixels where they are found in this new exposure (i.e., the system does not calculate to which pixels the telescope offset should have sent the stars, but rather assumes that the offset was applied correctly). Telescope offsets that are sufficiently small to keep the guide star on its CCD are accurate to at worst 1 arcsec.

2.5.3 Differential Guiding

For observations where non-siderial pointing is required, e.g. to follow or search for solar system objects, the telescope can be given a differential tracking rate. It is currently not possible to guide in this mode, either with the VST guide probe or with OmegaCAM. **Differential Guiding has not been fully commissioned and is not offered for the observing period P88.**

2.5.4 Image Analysis with OmegaCAM

The other two auxiliary CCDs are mounted out of focus. They intersect the stellar light beams in two planes, one in front of, and one behind, the focal plane. This gives information on the deviation of the beams from perfect cones with apex in the focal plane. Different kinds of aberration result in different shapes for these defocused stars, and this can be used to calculate corrections to be applied to the VST's active primary and secondary mirrors. Acquisition of the two image analysis stars, one per CCD, is designed to happen automatically, as does the computation of aberration coefficients. Image analysis is performed at the same wavelength as the autoguiding, which in most cases is the same as the science filter (see §2.3).

Image Analysis in the acquisition typically requires 3 iterations of 40 seconds each. During science exposures, aberrations are constantly measured by the IA system, and corrections are applied to the mirrors during the readout. The minimum science integration time that guarantees at least one aberration measurement is about 50 seconds. Image Analysis in the acquisition can be disabled for OB concatenations that perform a large number of observations back-to-back in adjacent fields.

2.6 Calibration lamps

Dome flat exposures can be taken with calibration lamps mounted at 90° intervals on the top ring of the telescope, illuminating a white screen on the inside of the telescope dome. The lamps are operated by carefully controlling the electric current, and their brightness is stable to about a percent over a timescale of several months.

Dome flat fields are used for monitoring the small-scale (pixel-to-pixel) variations in sensitivity of OmegaCAM, and for overall system throughput monitoring. Two sets of four lamps each are mounted

side by side. One set is used for routine daily calibrations, meanwhile the second set is cross-calibrated against the first at regular intervals. Once the lifetime of the first set of lamps has expired, its role is taken over by the second set, and the first set is replaced with new lamps. This procedure ensures a continuous record of throughput measurements, provides dome flat fields, and serves as a daytime health check.

2.7 Photometric Properties

Indicative magnitude zero points (the AB magnitude of a star that generates one electron per second) are given in Table 5. These numbers are consistent with the on-line Exposure Time Calculator (ETC)¹, which is based on the throughputs and reflectivities of the individual optical components.

Because of the way they are constructed, the OmegaCAM filters show some bandpass variation across the field. This variation is mostly axisymmetric, and it introduces a radially dependent colour term. Measurements will be included once they are available.

| Filter | Mag zero pt (AB) |
|-----------|------------------|
| <i>u'</i> | 23.9 |
| <i>g'</i> | 25.8 |
| <i>r'</i> | 25.7 |
| <i>i'</i> | 25.2 |
| <i>z'</i> | 23.8 |
| <i>B</i> | 25.7 |
| <i>V</i> | 25.5 |

Table 5: Magnitude zero points for the SDSS and Johnson filter sets. These are average values; chip-to-chip scatter is of order 0.1 mag.

2.8 Astrometric Properties

By design, OmegaCAM and the VST deliver a quite constant plate scale, and a rather uniform PSF. The radial plate scale is constant over the field to better than 1 part in 1000. The pixel scale with ADC in is 0.21506"/pix. With the ADC out – hence two-lens corrector in – it is 0.21343"/pix (theoretical value).

¹<http://www.eso.org/observing/etc/bin/gen/form?INS.NAME=OMEGACAM+INS.MODE=imaging>

3 Observing with OmegaCAM

To carry out observations with OmegaCAM, users need to prepare Observing Blocks (OBs) before the observations and submit those to ESO, using the Phase 2 Proposal Preparation (P2PP) system. More details on how to define OBs are given in §3.3. First the offsetting modes, and the effects of atmospheric refraction and dispersion, are described.

3.1 Offsetting Modes and Observing Strategies

3.1.1 Offsetting Modes

OmegaCAM observations can be taken with a number of *Offsetting Modes*: STARE, OFFSET, DITHER, or JITTER. They differ in the kind of offsets that are used between exposures, and in the final data product.

1. STARE: A sequence of N exposures of exactly the same part of the sky (except for the effect of differential atmospheric refraction, see §3.2.1). No offsets are done. To allow removal of cosmic rays by taking the median of images N must be at least 3.
2. OFFSET: A sequence of N exposures with almost full flexibility of offsets. Two limitations are to be considered. 1. Large offsets beyond the default dither pattern (Sect. 3.4.2) increase the overheads due to the need of guide star reacquisition. The execution time for offset sequences therefore increases by about 1 minute for each offset that goes beyond the default dither pattern (P2PP takes care of this calculation). This penalty will not apply if guiding is disabled in the acquisition, which is possible for short integrations of 1-2 minutes. 2. The maximum of a single offset accepted by the telescope is 1 degree in each of RA and DEC.
3. DITHER: A sequence of N exposures with offsets that are sufficiently large to bridge the gaps (up to 80 arcsec) between the CCDs in the detector mosaic. A DITHER observation results in an image which covers the field continuously, without large holes (provided $N > 3$). Some parts of the sky are seen by several CCDs, and all parts of the field are seen in at least $N - 2$ exposures.
4. JITTER: A sequence of N exposures with offsets that are sufficiently large (of order 1 arcsec) to shift cosmetic CCD blemishes to different parts of the sky. A JITTER observation results in a 32-fragment image (one fragment per CCD) in which the gaps between CCDs remain, but in which any part of the sky is seen by at most one CCD.

The pattern of offsets between successive exposures on a field distinguishes *dither* and *jitter*. They represent different trade-offs between trying to obtain data with uniform exposure level over the full OmegaCAM field, and trying to avoid having areas on the sky where data from different CCDs need to be combined. Such overlaps can give rise to discontinuities in the way the PSF varies across the field in the final stacked image, but this is unavoidable if the full field is to be exposed.

The key differences between the two modes are summarised in Table 6.

A number of patterns have been pre-defined for dither and jitter. They are described in more detail in the Template Manual [RD1].

Programmes that require very accurate PSF measurements should preferably use *jitter* as it results in a PSF which varies continuously over each CCD (except near the very edges)². *Dither* data should be used if the primary aim is to image a field completely.

²Note that, even though the CCD mosaic is extremely flat, significant jumps in PSF can still occur in coadded dithered images if the seeing varies from one exposure to the next.

| | JITTER | DITHER |
|---------------|--|-------------------------------|
| Correct what? | CCD blemishes only | also gaps in focal plane |
| Offsets | few arcsec | 25-100 arcsec |
| Data product | fragmented 1-square-degree-image | filled 1-square-degree image |
| Advantage | no combination of data from different CCDs | ~homogeneous exposure level |
| Penalty | gaps between CCDs | possible sharp changes in PSF |

Table 6: Key difference between the dither and jitter modes.

3.1.2 Observing Strategies

Observations are also taken under different *Observing Strategies*. Strategies are not implemented in ESO's Data Flow System, but may help the users in their own data reduction. The strategy used is written to the image headers (keyword TPL OBSSTRG).

Strategies extend beyond single OBs. The defined strategies are STANDARD, FREQ, DEEP, or MOSAIC. They can relate to how fields are laid out during observation preparation, and they can also provide specific instructions for data reduction, and for scheduling.

1. STANDARD: Used for a stand-alone OB, with no particular relation to other observations.
2. DEEP: Observations intended to generate a deep image, built up over several (typically many) OBs.
3. FREQ: Observations in which a field is monitored to form a time series. Specific time links (from minutes to months) may be specified for such observations as part of the OB preparation in P2PP. Specific time intervals can be specified for each OB; complex scheduling constraints, e.g. 'observe OB 1 five days after OB 2', can be specified in P2PP via time-links.
4. MOSAIC: Observations which will be used to map an area of the sky consisting of several (typically many) adjacent pointings.

3.2 Atmospheric Refraction and Dispersion

The atmosphere refracts light, as a result of which sources appear slightly closer to the zenith than they would be without the atmosphere. The effect is slightly wavelength dependent. This has two consequences: *atmospheric refraction* and *atmospheric dispersion*.

3.2.1 Atmospheric Refraction

A star's extra displacement r towards the zenith due to atmospheric refraction is given by

$$r = R \tan Z \quad \text{rad} \quad (2)$$

where Z is the zenith distance of the star, and R is the refractive index of air minus 1. To a good approximation

$$R \simeq 1 \text{arcmin}. \quad (3)$$

(R is slightly wavelength-dependent: see §3.2.2.)

Over the field of OmegaCAM, r takes slightly different values: from the center to the edge Z differs by $\delta Z = 0.5^\circ$, and so r varies by

$$\delta r \simeq R \sec^2 Z \delta Z \simeq 0.5'' \sec^2 Z. \quad (4)$$

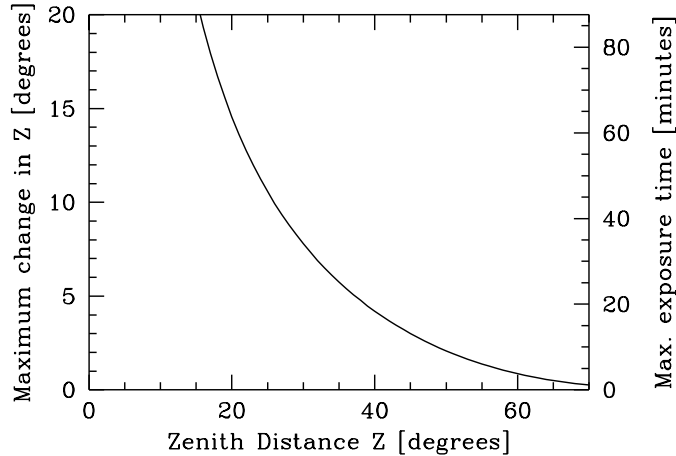


Figure 14: The maximum change ΔZ in zenith distance (degrees) that is allowed during an exposure before the image quality is degraded by 0.1 arcsec due to atmospheric refraction. The right-hand axis approximately translates this limit into an exposure time T (minutes) for a field on the equator, as seen from the Paranal latitude of -24° : $T = 4\Delta Z / \cos(-24^\circ)$.

Thus, the size of the field changes with zenith distance by an amount $2\delta r \simeq 1.0'' \text{ sec}^2 Z$. This is not a concern since the astrometric standard stars in the field suffer the same refraction, and so this effect is taken out in standard data reduction.

However, atmospheric refraction does affect long exposures at lower elevations. If δr changes significantly during an exposure then it becomes impossible to track objects in the center and outer parts of the mosaic at the same time (guiding with two stars will favour the center). As a result, image quality in the outer parts of the field will be degraded. The way to prevent this is to keep the exposures short, and so avoid a large change of δr during an exposure.

For δr not to change by more than 0.1 arcsec over an exposure requires

$$\delta(0.5'' \text{ sec}^2 Z) < 0.1'' \quad \text{or} \quad \delta Z < 6^\circ \cot Z \cos^2 Z. \quad (5)$$

At $Z = 45^\circ$, therefore, Z must not change by more than 3 degrees per exposure (for a target near the celestial equator this means no more than 12 min exposure); at $Z = 60^\circ$ the limit is below a degree change allowed (4 min exposure).

In poor seeing, or if image quality constraints are not so stringent, this limit can be relaxed and presents no practical concern.

Figure 14 shows a plot of the limit given by eq. 5.

3.2.2 Atmospheric Dispersion

Because refraction is wavelength dependent (more strongly so in blue light), the atmosphere turns objects into little spectra with the blue end pointed at zenith. Within the bandpass of a broad band filter this can cause image elongation and degradation. A model for the amount of atmospheric dispersion on Paranal has been calculated by E. Marchetti, see <http://eso.org/gen-fac/pubs/astclim/lasilla/diffrefr.html>. Based on these data, Table 7 shows the airmass at which atmospheric dispersion causes a smearing of the light over a 0.2 arcsec (1 pixel), 0.5 and 1 arcsec length. It is the responsibility of the user to specify the airmass constraints of their observations as a function of the filter used and the image quality requirements.

| Filter | Airmass at which dispersion reaches | | |
|--------|-------------------------------------|------------|----------|
| | 0.2 arcsec | 0.5 arcsec | 1 arcsec |
| u' | 1.05 | 1.22 | 1.75 |
| g' | 1.05 | 1.20 | 1.65 |
| r' | 1.20 | 1.90 | 3.35 |
| i' | 1.30 | 3.40 | > 5 |
| z' | 2.40 | > 5 | > 5 |

Table 7: The airmass (sec Z) at which the length of the atmospheric dispersion induced ‘spectrum’ reaches 0.2, 0.5 and 1 arcsec, for the SDSS filters.

Note that the ADC cannot be used in u' band, and that for P88 its use is discouraged since it has not been fully commissioned (see text).

To compensate the atmospheric dispersion effect, an Atmospheric Dispersion Compensator (ADC) was designed for the VST. It consists of two sets of counter-rotating prisms with which one can introduce given amounts of dispersion and thus cancel the atmospheric dispersion. The ADC has good throughput longward of 360nm wavelength; unfortunately this does not include the u' band³.

Important Note for P88. The ADC has not been fully characterised and commissioned yet. Therefore, its use is discouraged for P88.

3.3 OB preparation

Preparing an Observing Block is done with ESO’s P2PP tools. An OB consists of a number of templates, each of which represents a standard action taken by the telescope and/or instrument. Each OB should include one *target acquisition template*, whose main role it is to point the telescope at the target, and one or more *science templates* which perform the actual observation. In addition an OB contains a *constraint set* which specifies under which conditions (seeing, transparency, moon phase, timing constraints, ...) the OB may be executed. Full details are given in the P2PP instructions on the ESO web site [RD5].

For reasons of flexible scheduling of service mode observations at ESO, the execution time of each OB, including overheads, should be at most one hour. Longer observations need to be split into separate OBs. Unless there are good reasons to do otherwise, OBs should only use one filter each. If filter changes inside an OB are required, it is most efficient to order the exposures in such a way that filters are alternately selected from the two magazines. See Table 4 for the filter distribution.

To help with planning observations, one can use the Exposure Time Calculator (ETC) from the ESO web site.⁴

3.3.1 Target acquisition

A target acquisition presets the telescope pointing and configures the mirrors, corrector and instrument rotator. In addition it simultaneously prepares the instrument by loading the appropriate filter in the beam, and acquiring guide stars and image analysis stars if required.

³Note that the atmospheric extinction in u' is high, so observations in this band should in any case be taken as close to zenith as possible.

⁴<http://www.eso.org/observing/etc/bin/gen/form?INS.NAME=OMEGACAM+INS.MODE=imaging>

3.3.2 Scientific exposure

The scientific exposures load an appropriate filter, lock onto the guide and IA stars, perform any offsets, clear the CCD array, open the shutter for the appropriate time, close the shutter and read out the CCD array. A science template may command a number of exposures, possibly interspersed with offsets. Several science templates are needed if consecutive observations with different filters are required.

3.3.3 Dither and jitter patterns

Different templates are used for observations taken in dither or jitter mode. These templates implement different default offset patterns. The patterns are described in the Template Manual [RD1].

3.4 The Observing templates

The detailed use of the templates is described in a separate document [RD1]. Here the main functionality of the available templates is described.

3.4.1 Target Acquisition Templates

Each OB must start with an acquisition template, whose execution points the telescope and prepares the instrument.

Two acquisition templates are provided: `OMEGACAM_img_acq` and `OMEGACAM_img_acq_movetogap`. Each acquisition template allows specification of the object position, instrument filter for the first exposure, ADC or two-lens corrector (settings `COORD` and `NONE`, respectively), and Cassegrain rotator offset angle. It is also possible to specify whether or not autoguiding is required. Based on experience so far, unguided tracking for 60 seconds does not degrade image quality measurably. Finally, for OBs in concatenation it is possible to disable the start of Image Analysis in the acquisition.

The difference between `OMEGACAM_img_acq` and `OMEGACAM_img_acq_movetogap` is that the former acquires the field ‘blind’, while the latter takes a short exposure, which the operator can display and use to move the telescope so that a selected bright star falls in a gap between CCDs in order to reduce reflections and remanence.

3.4.2 Science Templates

Science templates perform the actual scientific exposure. For each of these templates the user must specify the exposure time and the filter to be employed, and optionally, the Observing Strategy used (see §3.1.2). The templates differ in the number and pattern of offsets that they use.

`OMEGACAM_img_obs_stare` takes a number of exposures through the same filter. The number of exposures, and the exposure time are specified. No offsets are made.

`OMEGACAM_img_obs_jitter` performs a jittered exposure (see §3.1.1). The number of exposures, the exposure times, and the step size for the jitter pattern can be specified. A step size of 1 arcsec suffices to correct for CCD blemishes and most dust particles on the detectors. If it is required that a given source is seen by a completely different set of pixels in each sub-exposure, the step size needs to be increased to above that of the sources. This is particularly true if accurate, real-time fringe maps need to be derived from the observations themselves. In those cases *dithering* may be more appropriate. The jitter template allows step sizes up to 100 arcsec but such large offsets are not recommended.

`OMEGACAM_img_obs_dither` performs a dithered exposure (see §3.1.1). The number of exposures, the exposure times, and the step size for the dither pattern can be specified. The dither patterns are designed to make sure the full field is observed, without gaps. Two step sizes can be given, one in X (along CCD rows) and one in Y (along columns). It is recommended that these are set to 25 and 85 arcsec, respectively, which are slightly larger than the largest gaps in the mosaic.

Two dither patterns are provided. The ‘diag’ pattern simply offsets in X and Y by the step sizes specified, resulting in a diagonal pattern of pointing centers. It results in an optimally homogeneous coverage of the field by the mosaic, for a given number of exposures.

The ‘starext’ pattern is more complex. It is designed to keep a small area of the field, containing a bright star, off the CCD array in order to reduce reflections. The size of this box area can be specified, recommended values are 8 arcsec \times 8 arcsec. Subject to that constraint this pattern yields the most homogeneous coverage of the field. It works best if the number of exposures is (a multiple of) 5. The move-to-gap acquisition template should be used with this template.

The dither and jitter patterns are illustrated in the Template Manual [RD1].

`OMEGACAM_img_obs_offset` allows full flexibility in the definition of offset patterns. The specified number of exposures are taken, and offsets are taken from a list. Offset data are processed in the same way as `OMEGACAM_img_obs_dither` data. Large offsets beyond the default dither pattern increase the overhead due to the need to reacquire a guide star. See 3.1.1 and the Template Manual [RD1].

3.4.3 Nighttime Calibration

A number of templates are provided for photometric zero point and atmospheric extinction measurements. Usually, these will be used by Observatory staff executing the calibration plan [RD2]; these OBs need not be specified as part of a science programme.

`OMEGACAM_img_cal_monit` takes an exposure of a standard field through the composite $u'g'r'i'$ calibration filter, using the two-lens corrector. This is typically done three times per night.

`OMEGACAM_img_cal_zp` takes an exposure of a standard field through any filter using the two-lens corrector. Twice per night an equatorial standard field is observed for the five filters $ugriz$. Furthermore, when science observations in user bands are done (B, V, v , Narrow Band filters), a standard field is observed in the respective filters.

3.4.4 Overheads

There are various overheads associated with OmegaCAM observations. Telescope preset to a new target typically takes about 2 minutes (slew speed better than 1 deg/s). Filter exchange in the instrument can be done at the same time; it takes between 65 and 115 seconds (the precise value depends on whether a filter is being swapped for another one from the same magazine, or whether they belong to different magazines). Acquisition of guide stars takes about 1 minute. A full IA sequence in the acquisition takes about 3 minutes. Successive bias frames can be read out every 40 sec, which covers the time needed to wipe the array, read it out and transfer it to disk (ordering the data into a FITS file takes place in parallel to taking the subsequent exposure).

Table 8 collects the currently known overhead values/best estimates.

| Constant | Value (seconds) | Remark |
|-------------------|-----------------|---|
| READOUT_TIME | 40 | Readout + Data written to disk |
| FILTER_SETUP | 65 or 115 | (see below) |
| TEL_PRESET | 120 | Slew_speed is a bit better than 1 deg/s. |
| TEL_OFFSET | 15 | [probably always absorbed in READOUT_TIME] |
| INS_GUIDESTAR | 60 | Total time for GS at the OB beginning. |
| INS_IASTAR | 180 | Time for IA at the OB beginning. |
| INS_GUIDESTAR_NEW | 60 | Acquire new GS after offset. |
| INS_GUIDESTAR_RE | 5 | Automatically reacquire same guide star after offset. |
| PICK_TIME | 45 | Time for pick object for MoveToGap acquisition. |
| ADC_SET | 160 | Time for deploying the ADC. |

Table 8: The various overhead times associated with OmegaCAM observations.

3.5 Survey Area Definition Tool

To help users in planning how to cover their target survey area a specific tool has been developed, the Survey Area Definition Tool (SADT).⁵ It is a mandatory tool for preparing survey observations with the Visible and Infrared Survey Telescope for Astronomy (VISTA), but it may also be used for preparing VST/OmegaCAM survey observations. The output of the SADT (survey area file in XML format) can be used together with the P2PP for Surveys to generate automatically large numbers of OBs.

A large survey consists of many 'tiles', or pointing centers. Observations of any type (stare, jitter, dither, offset) can be executed at a tile position. The SADT provides the tiles (and their central coordinates) that may be used to cover any given area of sky. Alternative ways of tiling the sky, e.g. the Astro-WISE 'PlateSystem' developed for the KiDS survey, may also be used but are not supported by the SADT.

3.6 Selecting exposure times and number of sub-exposures

The ESO website provides a link to the Exposure Time Calculator (ETC). It may be used to estimate signal-to-noise, count rates, etc., for OmegaCAM observations.

The sky background varies considerably with filter and with moon phase. The ETC gives the sky count rates per pixel at various moon phases. It is important to make sure that the read noise of the CCDs (about 5 electrons, equivalent to the noise of a 25 electrons per pixel background) does not add significantly to the sky background noise. Exposure times should ideally be such that the sky background is above 250 electrons per pixel. Particularly with the *u* and narrow band filters this requires minimum exposure times of several minutes, particularly in dark time.

3.7 Special features of the data

OmegaCAM data, as other wide-field CCD imager data, have several features that complicate data analysis. Data reduction software can cope with these, but it is important to be aware of them.

3.7.1 Point Spread Function

The focal plane of the telescope is not totally flat, such that even with perfect image analysis performed with the OmegaCAM auxiliary chip, mild PSF variations across the field-of-view are unavoidable. This

⁵For more information about SADT see <http://www.eso.org/sci/observing/phase2/SMGuidelines/SADT.html>.

'SF Anisotropy for frames with DATE-OBS 2011-09-03 02:29:07, filter SloanI (32 frame(s)), target=KIDS_339.0_-31.
Alt=62.385 Az=290.349 Rot=96.55557 Seeing=0.92 WindDir=200.0 Winsp=2.69

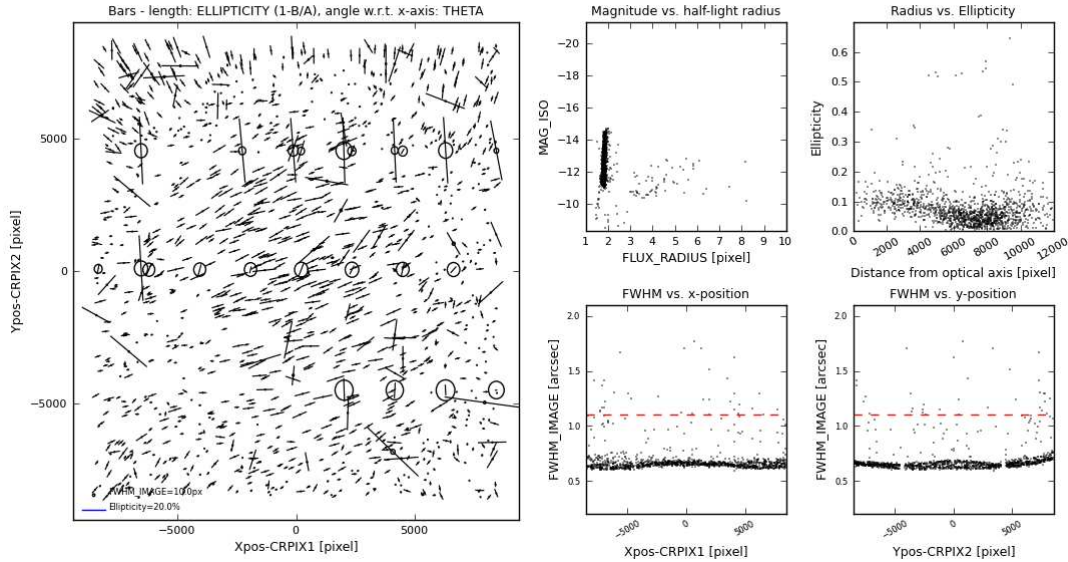


Figure 15: PSF anisotropy analysis plot obtained for an i-band observation. For the given example, outside seeing as indicated by the DIMM (around V-band) was $0.9''$, and IQ on OmegaCAM chips was $\sim 0.65''$. In general, IQ variations of up to 10-15% across the FOV can occur, depending on outside seeing, filter and telescope mirror position.

applies both to FWHM and ellipticity. In Fig. 15 we show a PSF anisotropy analysis plot obtained for a 240 seconds i-band exposure. In general, IQ variations of up to 10-15% across the FOV can occur, depending on outside seeing, filter and telescope mirror position.

3.7.2 CCD blemishes and particle hits

The OmegaCAM CCDs contain a number of cosmetic defects: hot pixels, cold pixels, and traps (see Table 1. The data on these pixels must be masked out before the data can be analysed; if such gaps in the data are unacceptable the observations need to be dithered, or at least jittered. Hot pixels and traps can result in entire columns of data being lost, so jitter/dither offsets must not be parallel to the CCD columns.

Some dust particles are also visible on the detectors: mostly these cover patches no more than about five pixels (1 arcsec) in size. At this point it is not clear whether/how often the dust particles move around.

In addition, particle hits on the CCDs release charge and obliterate small parts of the image. If these are a concern (their number grows with the exposure time) then several exposures are needed.

3.7.3 Ghosts and reflections

Unwanted reflections at air/glass interfaces result in some scattered light in the image. Some of these reflections are reasonably well-focused, resulting in 'ghost' reflections — spurious images from bright sources, appearing in different parts of the field. In OmegaCAM most of these ghosts are very defocused and hence very diffuse, but the most focused one projects to radii of a few mm and so is visible if there is a bright star in the field. It arises as a reflection off the entrance surface of the dewar window, followed by a reflection off the nearest filter surface. Another ghost arises as a reflection off the CCDs, followed by reflection at the entrance or exit surfaces of the dewar window. (These

reflections disappear when the star falls on a gap between CCDs.)

By way of example, Fig. 16 shows the four main reflections from a bright star on CCD #91. The associated table lists typical size and surface brightness (relative to the bright star) of these ghosts. Note that the sizes and positions of the ghosts depend on the location of the parent star in the image, and their brightnesses on the filter in use.

Ray tracing calculations predict that a bright star at distance R° degrees from the center of the field will have a ghost that is displaced radially outwards by

$$21''R^\circ + 70''R^{\circ 3} \quad (6)$$

and that this ghost has a diameter of

$$23'' + 73''R^{\circ 2}. \quad (7)$$

In some cases, reflections from stars outside the field are seen. Their origin is still under investigation. Initial results are that these are caused by bright stars which lie between 0.5 and 0.53 degrees E or W (in the default orientation of the mosaic) of the pointing center, in the top or bottom row of CCDs. The reflections are linear, narrow features perpendicular to the edge of the mosaic. An example is shown in Fig. 17. Stars outside the top and bottom edges also cause linear reflections, but less frequently. They require a star 0.56–0.565 degrees N or S of the pointing center. These reflections are weaker and less focussed than the previous ones. Their cause is also still under investigation.

3.7.4 Sky concentration

Multiple reflections also generate a very defocused image of the field, which is added to the sky background in the image. The effect, usually referred to as ‘sky concentration’, is a smooth, additive component to each image.

The additive term is also present in flat fields, be it from the sky or from an exposure of the dome screen. If this additive term is not subtracted from the flat fields first, the result of flat-fielding is an image with a flat background but a varying photometric zero point.

Determining such a ‘photometric flat field’ is best done by observing large standard star fields. Note that one way to mitigate the effect is to calibrate each exposure CCD by CCD, since the pattern is expected to be dominated by scales larger than an individual chip.

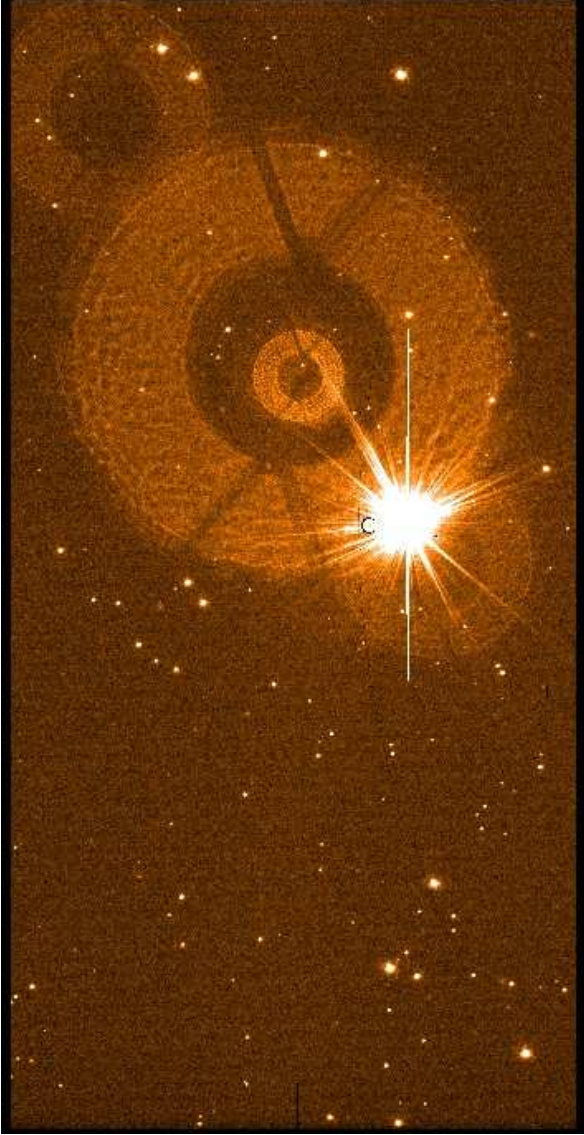
Sky concentration has been shown in the commissioning to be up to 15% in the g-band, and less in the other Sloan bands and the Johnson bands. More precise numbers will be provided in the next Manual edition for P89.

3.7.5 Diffraction Spikes

The spider that holds the secondary mirror in place causes diffraction spikes around bright stars. Because the VST is an alt-az telescope, the camera rotates with respect to the spider during an exposure, causing this spike pattern to rotate as well.

3.7.6 Fringes

Internal reflections in the CCD and the consequent interference gives rise to fringes in the sky background. These effects show up in the i' and z' bands (and to a low extent in r'), and can have amplitudes up to $\sim 10\%$ in z' band. The fringes are caused by the emission lines in the night sky spectrum, and can be highly time-variable. As the equivalent width of these lines varies in the sky spectrum so do the fringe amplitudes and to some extent the patterns. This additive effect is mapped



| Ghost | radius (arcsec) | surf.br. $\Delta\text{mag}/\text{arcsec}^2$ | remark |
|-------|--------------------|--|------------------|
| 1 | 70 | 16 | window/filter |
| 2 | 330 | 16.6 | CCD/outer window |
| 3 | 150 | 17.1 | CCD/inner window |
| 4 | 160 | 17.6 | window/filter |

Figure 16: Example ghost reflection from a $g = 6.5$ magnitude star in a 60-second g band exposure. The ghosts line up along a radius vector through the center of the array, which is towards the bottom right in this case. Ghosts are numbered in order of decreasing surface brightness: from top bottom, numbers 4,2,1,3. The table on the right gives their radii and surface brightness, scaled to a magnitude zero parent star.

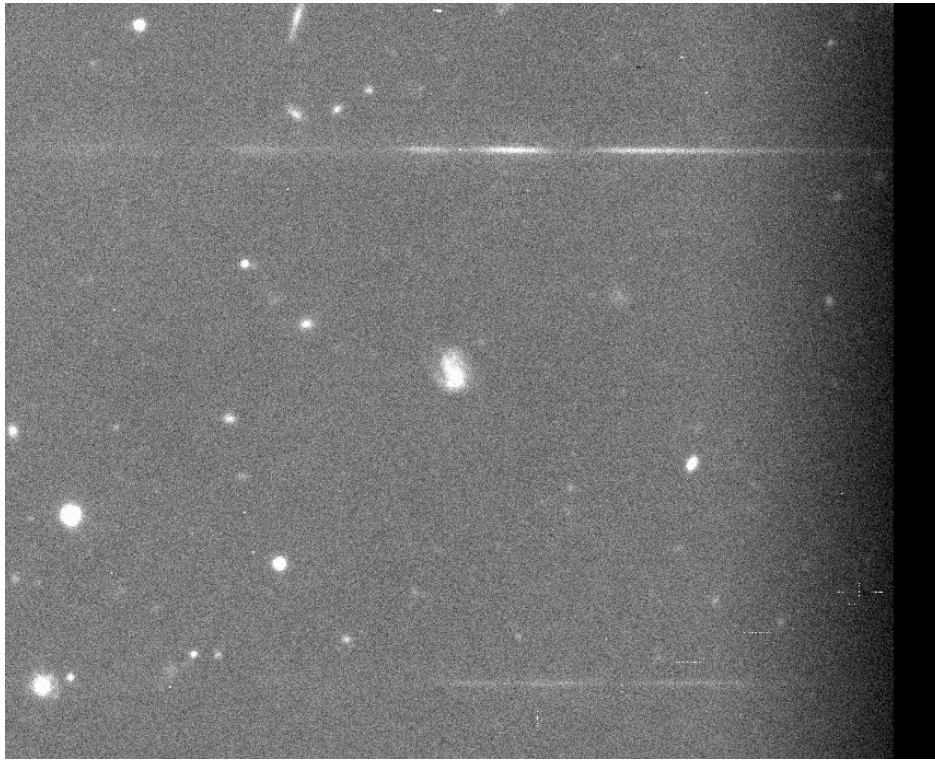


Figure 17: Example of reflection of light from a star (in this case, two stars to the West) outside the field. Such features can occur on each of the four corner CCDs.

by comparing twilight sky exposures (with relatively weak sky emission lines) with dark sky exposures. Appropriately scaling this ‘fringe map’ to individual exposures then allows the fringe pattern to be subtracted.

3.7.7 Remanence

Exposure to a very bright star can saturate the CCD, and can leave a surplus of charge on the surface of the detector. This can take some time to diffuse away, and meanwhile any subsequent readouts will show a faint residual of the saturated star. Such remanence can take well over half an hour to decay away.

3.7.8 CCD Crosstalk

CCDs ## 93-96 are known to suffer some electronic crosstalk. Since crosstalk has not been found down to very low levels in any of the other CCDs, the explanation lies either in the CCDs concerned themselves or some manufacturing problem of the detector-head electronics. There are no current plans to take remedial action as any intervention in the detector head entails a high risk.

The crosstalk has its origin in bright objects. The threshold for triggering crosstalk depends on the CCD and time. Mostly it requires saturating the A/D converter, but also unsaturated sources can lead to electronic ghosts in other CCDs, at a level of up to 0.4% of their ‘parent’. These ghosts look like real sources and cannot be removed by dithering.

The crosstalk can be both positive (bright) and negative (dark) with a range of up to 0.4%; it is generally weaker the larger the distance between source and target CCD is. The ghost images always occur at the same relative pixel coordinates in the target CCD, at which the star in the source CCD

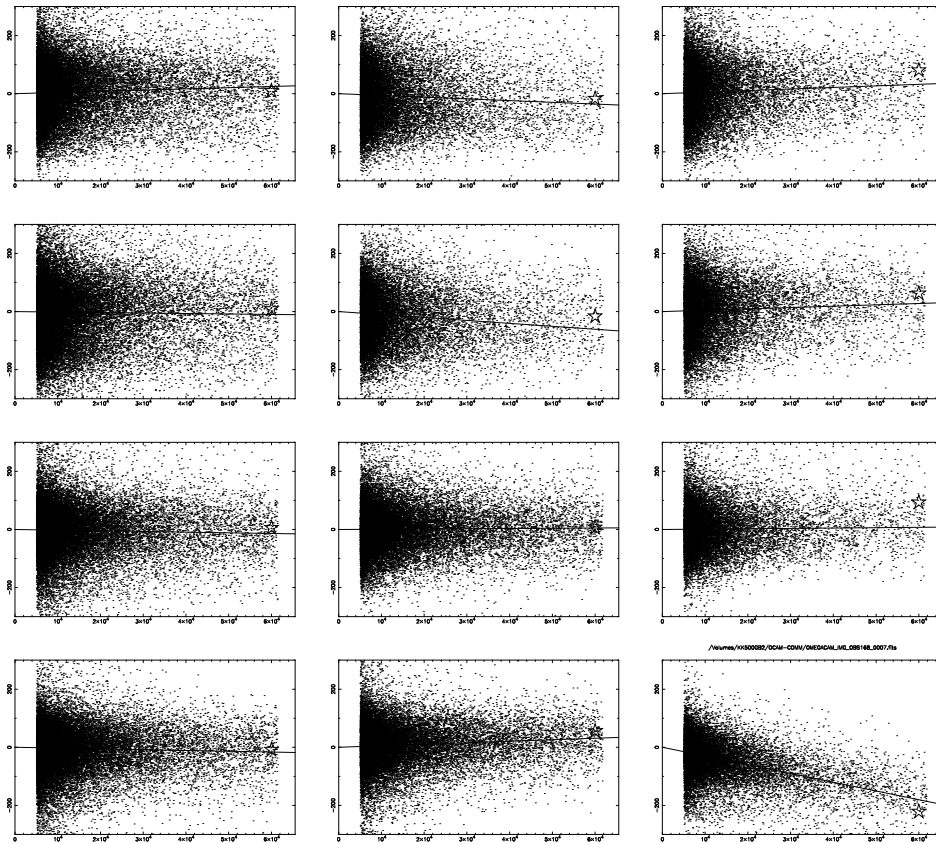


Figure 18: Crosstalk between CCDs 93–96. Each panel shows the counts in a raw frame of a 'receiver' CCD as a function of the counts in another 'emitter' CCD. In several cases there is a clear linear relation, illustrating crosstalk from unsaturated pixels. Saturated pixels also cause crosstalk in many combinations of emitting and receiving CCD: their median count level is shown as a star. Each row corresponds to a different receiver CCD; within a row the three possible emitter CCDs are plotted in numerical order.

is located.

The crosstalk pattern present in any image consists of several sub-patterns (see Fig. 18). The most common ones are:

(i) Negative crosstalk from #96 to #95. This is always present. (ii) Positive crosstalk from #94 to #95 and on to #96. It seems that #95 may sometimes be skipped over. (iii) Positive crosstalk from #96 to #95 to #94 and, very rarely, to #93.

Dedicated data reduction procedures to flag or remove these artefacts are under development.

The effect of this crosstalk on the flat fields is still to be investigated in detail.

4 Calibrating and Reducing OmegaCAM data

All OmegaCAM data are taken in service mode, in the context of a calibration plan [RD2] whose function is to maintain the overall calibration of the instrument and atmosphere. Thus the aim is not to calibrate individual data sets, but rather to calibrate the telescope+instrument+sky chain.

Data volumes from OmegaCAM are LARGE. A single exposure leads to 0.5Gbyte of raw uncompressed data (at 2 bytes per pixel); processed exposures, with a 4-byte real number per pixel, are over a gigabyte in size. Typical data volumes from a single night are 30-60 Gigabytes of raw science data; another 30-40 Gbyte of raw calibration data are also taken every day.

OmegaCAM data are processed using a pipeline (see [RD3] for a full description) which is run by the ESO Data Flow Operations group, and is used for quality control purposes. On Paranal, a special version of the pipeline is running for real time QC0 checks of image quality (FWHM, ellipticity) and sky transparency. Only raw data is made available to the general user.

All data from OmegaCAM are delivered as multi-extension FITS files. The first extension contains the observing parameters, and extensions 2–33 contain the data from the individual CCDs. Note that the name of the CCD, as identified in Fig. 4 is included in the header of the corresponding FITS extension. The order in which extensions appear in the FITS file may vary and should *not* be relied upon to identify CCDs.

4.1 Calibration Plan

The full details of the calibration plan are given in a separate document [RD2]. From the point of view of planning or preparing observations with OmegaCAM, we summarise the important features here.

Bias, dark and flat field exposures are taken with a frequency to be determined by experience: currently biases are taken daily, dome flats every three days, and darks weekly. In clear conditions, sky flats are taken every night in 2-3 filters. One can hence expect each key band to have sky flat every 3 days. Master flat fields are derived from a combination of twilight and dome flats. Fringe maps are derived by comparing these flat fields to night-sky exposures.

The photometric zero point is determined as follows. The basic approach is that the atmospheric transparency and instrument efficiency are monitored several times per night in four of the SDSS bands ($u'g'r'i'$, the so-called *key bands*) using the two-lens corrector, whereas other filters (so-called *user bands*) are cross-calibrated against these. All filters, including $u'g'r'i'$, are considered as *user bands* when they are used in combination with the Atmospheric Dispersion Corrector (ADC).

OmegaCAM employs a 4-quadrant calibration filter, which is used to monitor the sky transparency and the instrument zero point in $u'g'r'i'$ bands simultaneously. At least three times a night, a standard star field on the celestial pole is observed with this filter to measure atmospheric extinction. In evening twilight and around midnight a high-elevation standard star field is observed with this same calibration filter, and with the monolithic science filters from the SDSS system. A standard for the user bands used on a particular night is also observed close in time to the science observation.

Figure 19 shows schematically with what frequencies calibration data are taken.

Astrometric calibration is performed by reference to the many USNO catalogue⁶ stars that are present on each CCD. No special calibration observations are needed. With the broadband $g'r'i'z'$ filters and exposure times between 10 seconds and 10 minutes the USNO stars should be unsaturated. Short u' band observations (less than a minute) may not provide sufficient stars for an accurate astrometric

⁶The USNO astrometric star catalogues contain over 400 million stars over the whole sky (an average of 10,000 per square degree, or 300 per OmegaCAM CCD), down to ~ 20 th magnitude in R . Typical astrometric uncertainty for each star is $0.3''$ rms. More information on the catalogue can be found at <http://archive.eso.org/skycat/usno.html>.

Monitoring the Photometric Calibration

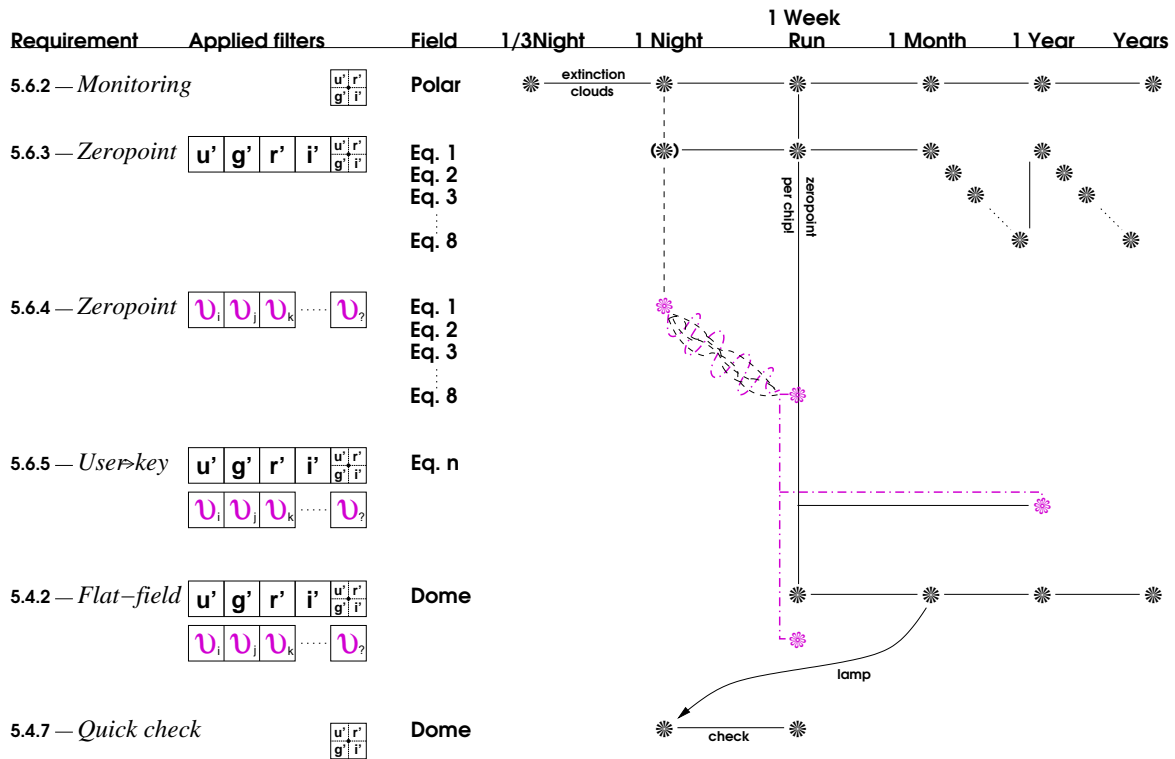


Figure 19: The frequency with which the various types of calibration data are taken. More details are given in the Calibration Plan [RD2]. The symbol \mathcal{U} denotes a user band.

solution.

More specialised calibration files, related e.g. to sky concentration, or fringing from night-sky lines, are derived from the observations themselves, or from less frequent dedicated measurements.

The calibration plan is specified to deliver photometric zero points accurate to 0.05 magnitudes, and astrometry with rms error 0.1 arcsec, in a fully automatic pipeline reduction mode.

4.2 Data reduction Pipeline

Data delivered to the ESO archive consist of the raw exposures, as well as the calibration data. The header of the image contains the astrometric world coordinate system. The photometric zeropoint is provided as a separate calibration file.

The pipeline performs the following main steps, using calibration files derived by the ESO Data Flow Operations Group in Garching:

1. Each CCD frame is debiased
2. Bad pixels are flagged
3. Cosmic rays and satellite tracks are detected and flagged.
4. Data are divided by a normalised flat field image
5. If appropriate, fringes are removed
6. An astrometric solution is computed for each CCD based on a search of USNO stars in the image
7. Images are background-subtracted, corrected for sky concentration and resampled to a common, linear world coordinate system.
8. Different exposures in the same template are combined. Data taken in DITHER/JITTER/OFFSET mode are combined into a single image covering the full field of view, taking into account weights and bad pixel masks. STARE mode data are processed into 32 series (one per CCD) of calibrated exposures without co-addition.

4.3 Quality Control

ESO performs real time quality control during the observations, using QC parameters derived by the data reduction pipeline. The main parameters used in real time QC (named QC0 on Paranal) are FWHM, ellipticity of point sources in the science images, and photometric ZPs derived from standard star exposures. For each exposure and each of the 32 CCDs, the above QC parameters are provided as pipeline output and queried with scripts by the nighttime operators. Image Quality average is contrasted with the user requirements to determine whether an executed OB is within constraints. Also, ellipticity and image quality degradation across the FOV are monitored.

All OmegaCAM data are transferred to Garching via USB disks. In the medium term future it is envisaged to transport the data via a fiber link between Paranal and Antofagasta (EVALSO) to Europe, such that the delay will only be a few hours at most. Health checks of the calibration data are performed by the Quality Control Group in Garching to monitor the status of the instrument. The link to the health check pages is http://www.eso.org/observing/dfo/quality/OMEGACAM/reports/HEALTH/trend_report_BIAS. A scoring scheme is applied to those QC parameters. Also the Paranal pipeline provides health check parameters which can be scored to monitor the instrument status. Also, about 10% of the scientific data are analysed by Quality Control in Garching.

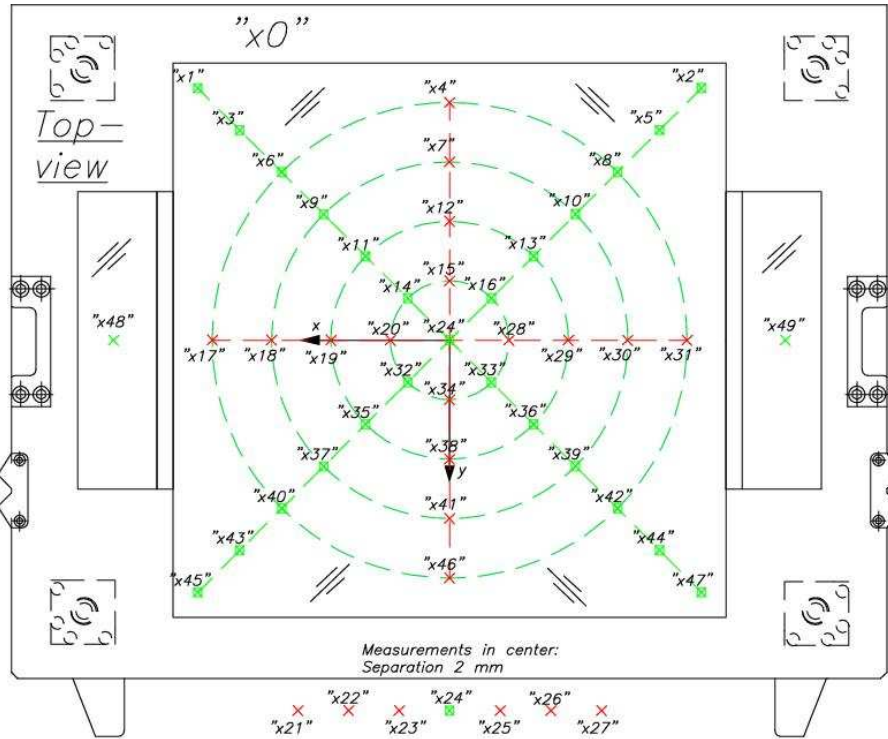


Figure 20: Location of the filter throughput measurements and coordinate system definition. The concentric circles have radii of 29, 57.5, 86, and 115mm; additional measurements on the diagonals were made at radii of 144 and 172mm. The x and y coordinate axes are indicated; the filter moves towards its positive y (with the two notches ahead) when it is inserted in the instrument. The filter coordinate system is identical with the instrument coordinate system if the filter is loaded from magazine B.

A Filter throughput curves

In this section we present the results of measurements of the filter throughput, performed in the lab at the Universitäts Sternwarte München.

A.1 Broad band Sloan filters (ugriz)

As described in §2.3, the Sloan filters are interference filter sandwiches. Because of the manufacturing process, and because the beam of the telescope crosses the filters under different angles in different parts of the image (see Fig. 2), the bandpass of the filter is slightly field dependent. The laboratory measurements were designed to mimic the converging, tilted beam from the telescope as a function of position in the focal plane.

Below we provide fitting formulae for the radial variation of central wavelength, blue edge and red edge of each filter, as well as plots of the filter profile at the center of the filter. Apart from the wavelength shift, the shape of the filter response is rather constant with field position. *The filter response curves have all been multiplied by the average quantum efficiency of the OmegaCAM CCDs.*

In the case of two filters (i and r), the bandpass variation was not quite axisymmetric about the physical centre of the filter. For these a best-fit center was determined; the location of the center is reported in §A.4.

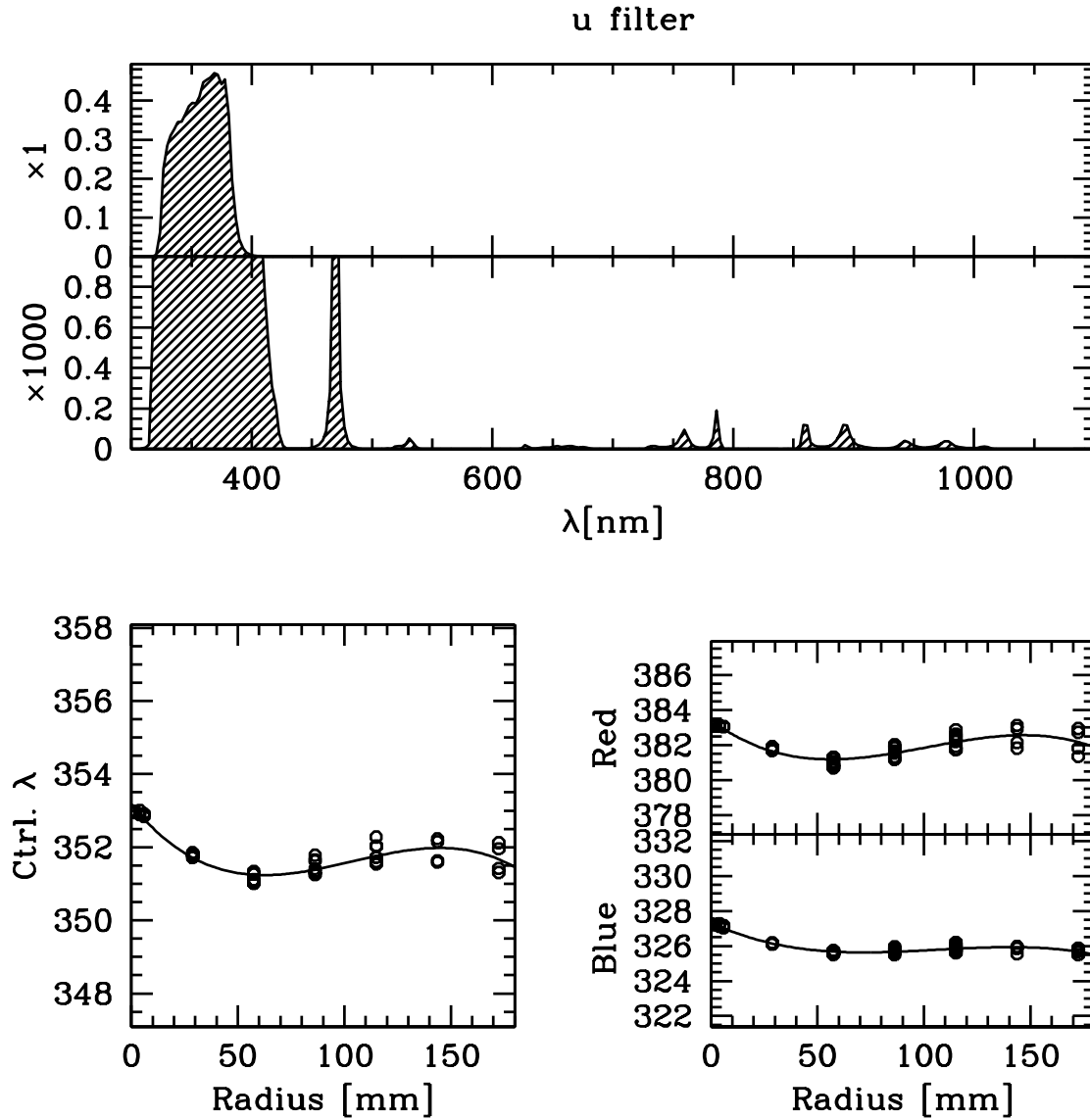


Figure 21: Top panels: throughput of the u filter \times average CCD response curve, including a blow-up by a factor of 1000 to show the out-of-band blocking. Bottom left: variation of central wavelength with radius on the focal plane (dots: measurements; line: polynomial fit). Bottom right: corresponding variation of wavelength at half-maximum throughput of the blue and red edges of the filters.

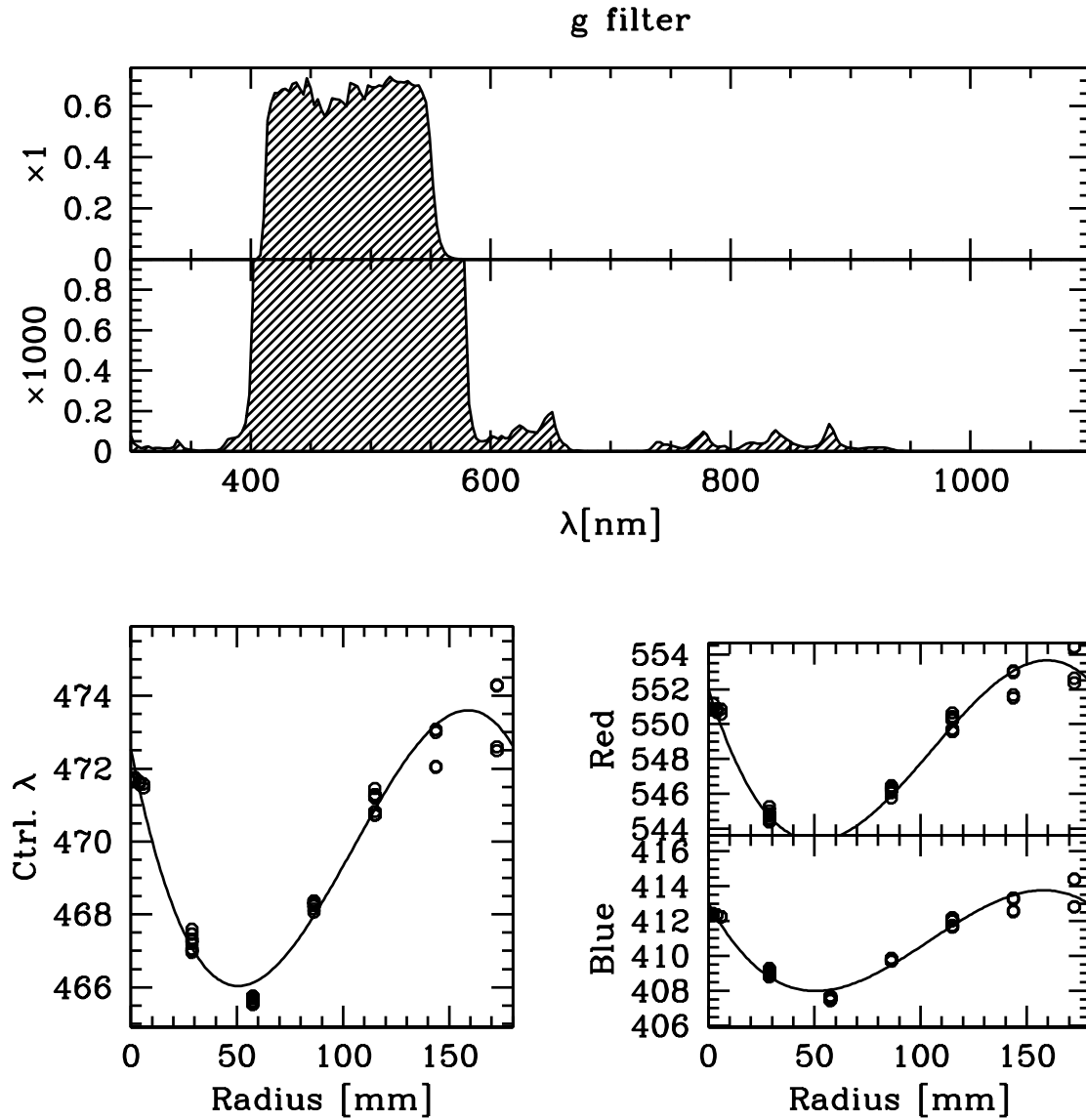


Figure 22: Top panels: throughput of the g filter \times average CCD response curve, including a blow-up by a factor of 1000 to show the out-of-band blocking. Bottom left: variation of central wavelength with radius on the focal plane (dots: measurements; line: polynomial fit). Bottom right: corresponding variation of wavelength at half-maximum throughput of the blue and red edges of the filters.

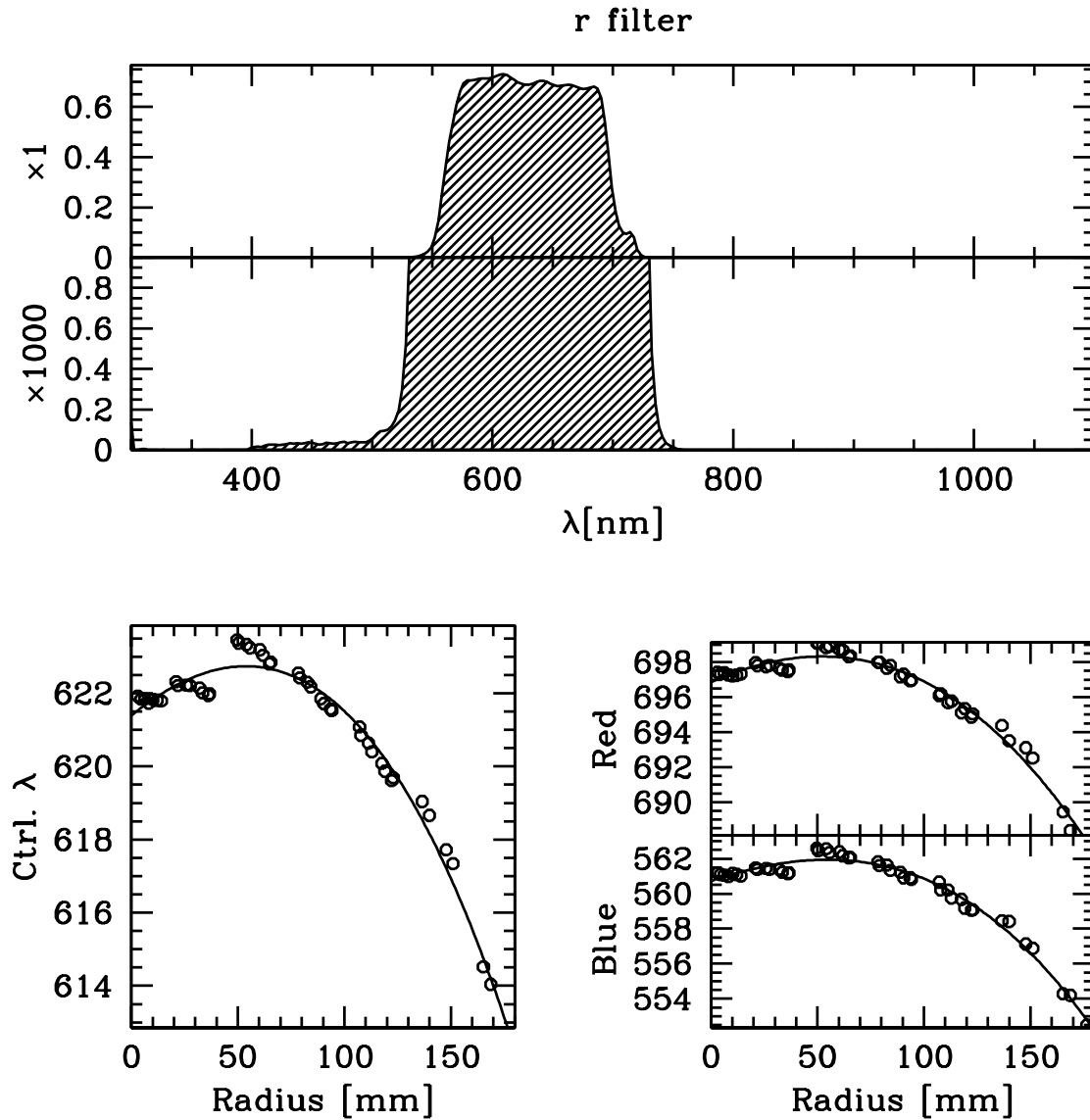


Figure 23: Top panels: throughput of the r filter \times average CCD response curve, including a blow-up by a factor of 1000 to show the out-of-band blocking. Bottom left: variation of central wavelength with radius on the focal plane (dots: measurements; line: polynomial fit). Bottom right: corresponding variation of wavelength at half-maximum throughput of the blue and red edges of the filters. Note that for this filter the bandpass variation is most symmetric about the an offset center—see §A.4.

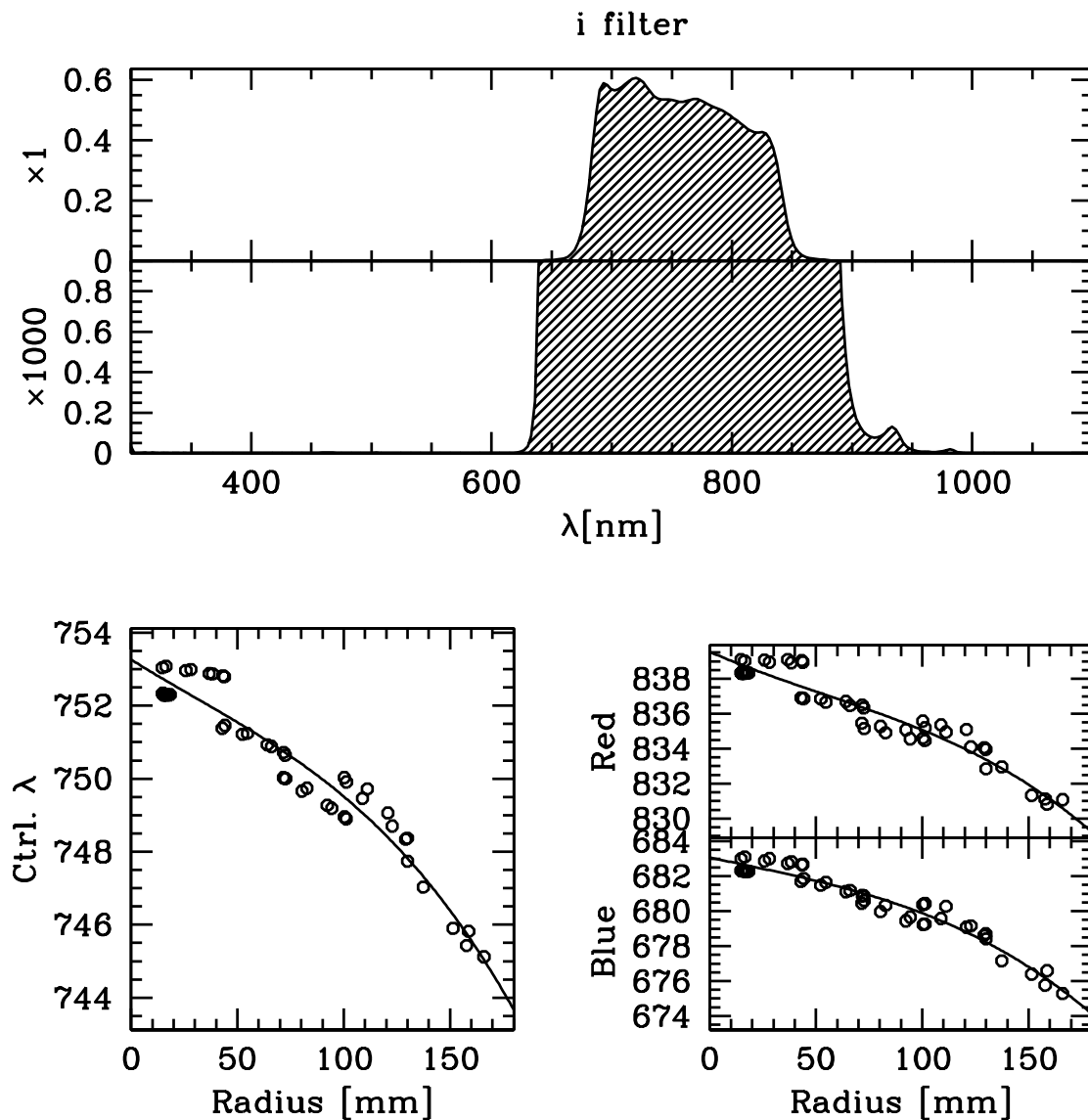


Figure 24: Top panels: throughput of the *i* filter \times average CCD response curve, including a blow-up by a factor of 1000 to show the out-of-band blocking. Bottom left: variation of central wavelength with radius on the focal plane (dots: measurements; line: polynomial fit). Bottom right: corresponding variation of wavelength at half-maximum throughput of the blue and red edges of the filters. Note that for this filter the bandpass variation is most symmetric about the an offset center—see §A.4.

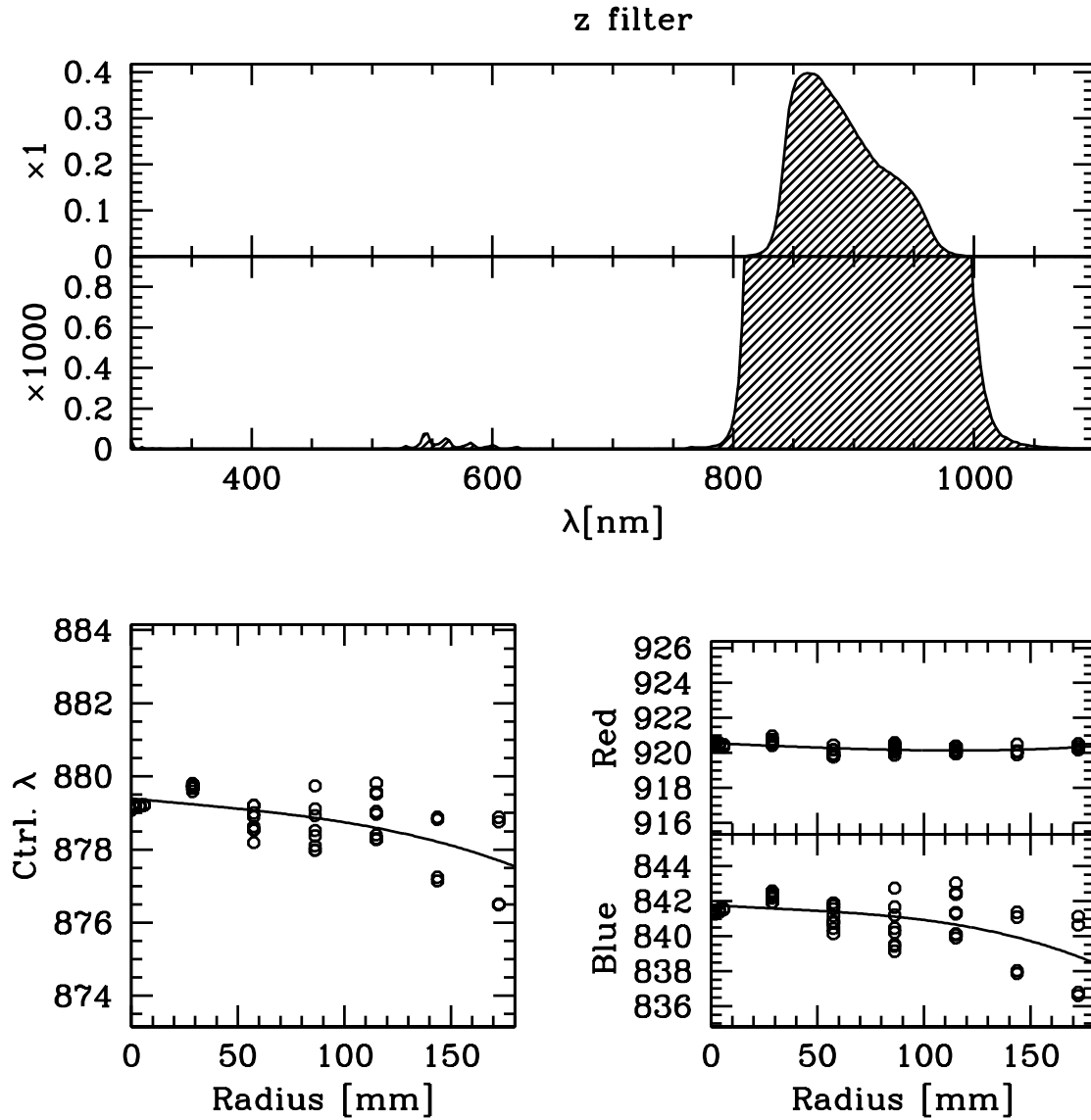


Figure 25: Top panels: throughput of the z filter \times average CCD response curve, including a blow-up by a factor of 1000 to show the out-of-band blocking. Bottom left: variation of central wavelength with radius on the focal plane (dots: measurements; line: polynomial fit). Bottom right: corresponding variation of wavelength at half-maximum throughput of the blue and red edges of the filters.

A.2 Segmented Broad-band filters (Johnson B and V)

TBD for P89

A.3 Narrow-band filters (Strömgren v and $H\alpha$)

TBD for P89

A.4 Radial variations in bandpass

The radial variation of central and half-power wavelengths, expressed in nm, can be described as the sum of the following polynomial terms in r [mm]:

| u | | $\times 10^{-2}r$ | $\times 10^{-4}r^2$ | $\times 10^{-6}r^3$ |
|-----------|-------|-------------------|---------------------|---------------------|
| Central | 353.2 | -7.24 | 8.29 | -2.66 |
| Blue edge | 327.3 | -5.71 | 6.01 | -1.89 |
| Red edge | 383.4 | -9.15 | 11.27 | -3.70 |

| g | | $\times 10^{-2}r$ | $\times 10^{-4}r^2$ | $\times 10^{-6}r^3$ |
|-----------|-------|-------------------|---------------------|---------------------|
| Central | 472.5 | -28.72 | 37.43 | -11.91 |
| Blue edge | 413.0 | -22.29 | 29.10 | -9.30 |
| Red edge | 552.0 | -38.51 | 50.15 | -15.90 |

| r | | $\times 10^{-2}r$ | $\times 10^{-4}r^2$ | $\times 10^{-6}r^3$ |
|-----------|-------|-------------------|---------------------|---------------------|
| Central | 621.4 | -4.72 | -3.55 | -1.05 |
| Blue edge | 560.7 | -4.07 | -2.74 | -1.20 |
| Red edge | 696.9 | -5.42 | -4.57 | -0.81 |

Note: Radius cf. position (-7.9, -2.3)

| i | | $\times 10^{-2}r$ | $\times 10^{-4}r^2$ | $\times 10^{-6}r^3$ |
|-----------|-------|-------------------|---------------------|---------------------|
| Central | 753.3 | -3.64 | 0.93 | -1.04 |
| Blue edge | 683.1 | -2.62 | 0.35 | -0.93 |
| Red edge | 839.5 | -5.29 | 2.14 | -1.33 |

Note: Radius cf. position (4.8, 14.8)

| z | | $\times 10^{-2}r$ | $\times 10^{-4}r^2$ | $\times 10^{-6}r^3$ |
|-----------|-------|-------------------|---------------------|---------------------|
| Central | 879.4 | -0.58 | 0.16 | -0.22 |
| Blue edge | 841.8 | -0.81 | 0.61 | -0.66 |
| Red edge | 920.6 | -0.52 | -0.04 | 0.16 |

Where the radius is referred to an offset centre, its location is given in the (x, y) coordinates shown in Fig. 20.

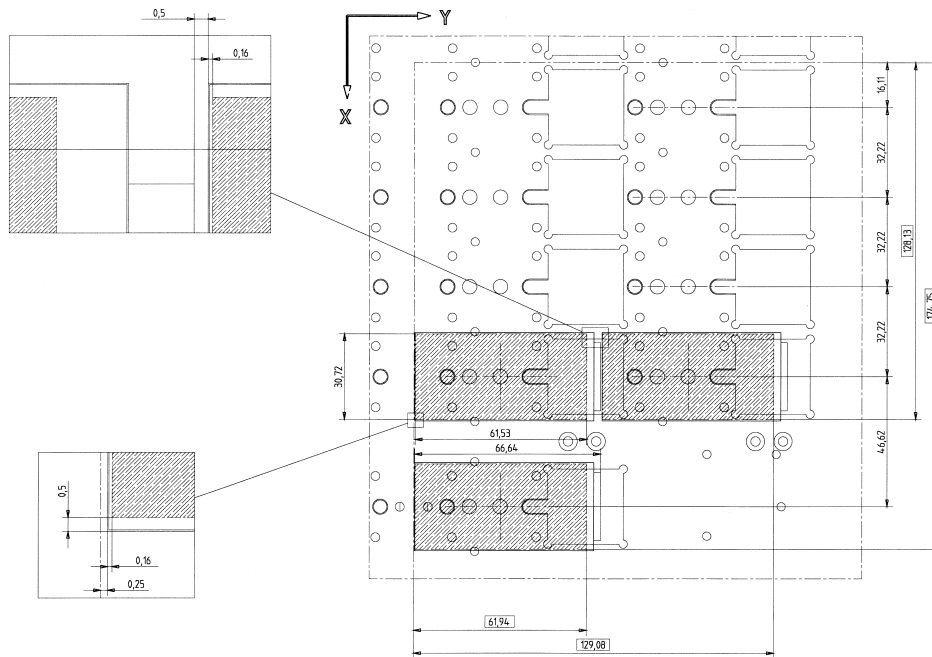


Figure 26: Technical drawing showing the pixel positions in the array.

B Layout of the CCDs in the mosaic

The unit CCDs are mounted in the science array as closely as possible. This is illustrated in Fig. 26. The resulting gap sizes are:

- between the long sides of the CCDs: 1.5mm (100 pix)
- central gap along the short sides: 0.82mm (55 pix)
- wide gap along short sides: 5.64mm (376 pix)
- between science array and auxiliary CCDs: 15.9mm (1060 pix)

C Detector response curves

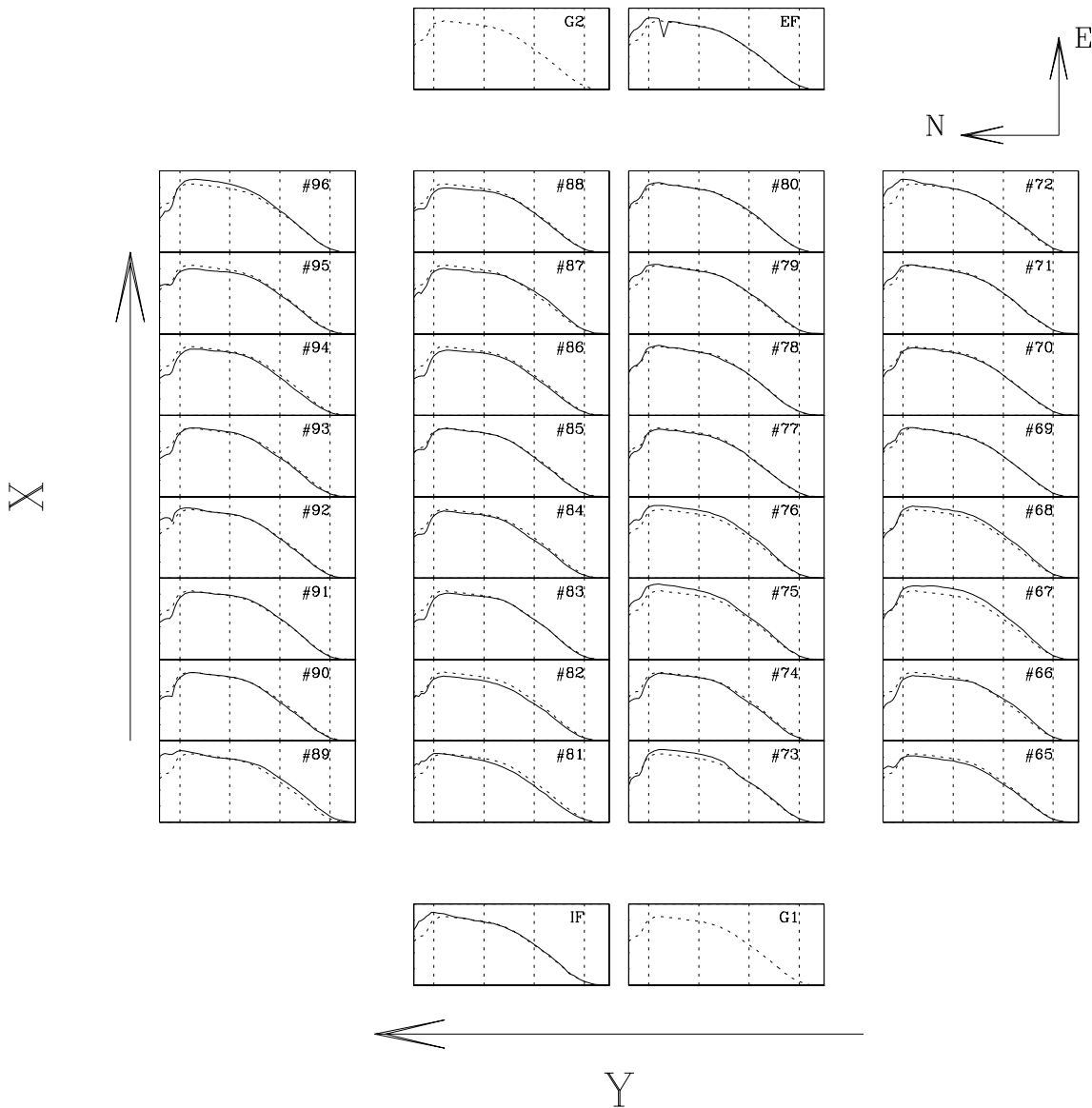


Figure 27: The QE curves for all CCDs in the mosaic, laid out as the mosaic itself (top view). The solid curve in each panel is the measured QE for that device; the dotted curve is the average for all 32 science CCDs. The wavelength range from 320 to 1100nm is plotted; dotted lines indicate 400, 600, 800 and 1000nm. X and Y are coordinates in the focal plane; for the default instrument rotator position angle of 0 X points East and Y points North.

The CCDs labelled IF and EF are the intra- and extrafocal CCDs, for image analysis: these are mounted 2mm above and below the rest of the CCDs, respectively. G1 and G2 are guider CCDs.